Response to the comments of Anonymous Referee #1

Referee General Comment:

In this manuscript, the authors develop parameterizations of the glass transitions temperature (T_g) based on vapor pressures of a large number of pure organic compounds containing C, H, N, O, and S. The authors compare T_g predictions based on several different algorithms and then use the algorithm to predict the phase of SOA based on SOA volatility measurements from field studies. Finally, the impact of condensed phase water on the aerosol viscosity is examined. Calculations of the phase of organic aerosol is timely, relevant, and will be of interest to readers of ACP. The number of figures is appropriate and are generally well presented. The writing is clear and generally well organized, though could use some further technical editing. The authors are attempting to reduce a very challenging problem in the field to a parameterization that can be reasonably included in a global modeling framework with limited data to work with. I applaud them for this effort and fully recognize this is challenging, particularly with the limits in the data. With that said, I think the authors could have done a better job in more clearly addressing the uncertainties and limitations in the inputs to their parameterization early in the manuscript. In addition, large number of parameterizations and different data analysis and parameter estimation methods gets confusing at times. These points can be remedied with relatively minor revisions. Perhaps more challenging is that the results of the parameterization themselves don't seem to constrain the phase of OA particularly well. One example from the text is that for the SOAS campaign the range of T_g for OA is between 232 – 330 K depending on how the same set of data is analyzed. So, a reader (or reviewer) may be either confused or left wondering what exactly these calculations tell us. Adding condensed phase water and its impact on phase/volatility further increased the complexity. I suggest the authors try to better address this uncertainty/error/prediction range more thoroughly. I don't expect they will be able to resolve the issue and I don't have any specific suggestions for how to resolve this, but I think the attempt would significantly improve the impact of the paper. After these corrections, the manuscript would be appropriate for publication in ACP.

Response: We thank Anonymous Referee #1 for the positive review and very helpful suggestions. Following your suggestions, we have improved the writing in the revised manuscript and added some statements to prevent an abrupt transition between different sections. We add a new subsection 2.1 "Dataset of glass transition temperature" to describe the training and test datasets and address the uncertainties and limitations in the inputs (see our response to your comment 3). We also divide the Method section into three subsections and keep the main parameterization predicting the glass transition temperature as a function of volatility in the main text. We move other parameterizations and related comparisons to the Appendix (see our response to your comment 1). In addition, we re-organize the paragraphs about the T_g of total OA at the dry condition ($T_{g,org}$) during the SOAS campaign and clarify that the most credible predicted $T_{g,org}$ values span in the range of 313 – 330 K (see our response to your comment 1). We also clarify the reasons why we predict the viscosity at different relative humidity and the relative importance of volatility and particle phase water in

OA phase state predictions (see our responses to your comments 1 and 5). We believe after addressing the above major issues, the take-home messages of this manuscript are clearer. Please see the detailed responses below.

Referee Major Specific Comment:
(1) Improve clarity of the presentation and take-home message.

I had to read the manuscript several times to fully understand the method the authors were using. One challenge is that at least 5 different T_g parameterizations are presented and compared (Eqs. 1, 2, 3-5, 6, and a global model parameterization), and it gets difficult for even a careful reader to keep track them. A few suggestions to improve this: 1) label the figures themselves (i.e. in a title) so the reader doesn't have to study the caption to understand the figure, 2) shorten the captions to be more concise; the key figures have captions that are a paragraph long, 3) refer to the parameterizations by a descriptive name rather than the equation number (for example, Volatility + O:C, Volatility only, composition only, global model); this is done some places in the manuscript, but not all.

Response: Following your suggestions, we have (1) added titles in Fig. 1, Figures in the Appendix and Figs. S3-5; (2) shortened the captions of all figures in the main text and the supplement; (3) referred to the parameterizations by descriptive names through the manuscript. In addition, we have moved the parameterizations as a function of elemental composition and the comparison with the parameterization in Zhang et al. (2019) to the Appendix for better readability of the main discussion.

In addition, there are (at least) 4 different methods to infer aerosol volatility, at least 2 methods of "measuring" T_g, and possibly different ways of "measuring" T_m. Again, it got difficult to track what measured as opposed to calculated and what was being compared, given the large number of combinations and permutations of T_g, T_m, volatility, etc. involved. One example: in Figure 3 the x axis is labeled "Measured T_g" while in Figs 1 and 2 it is labeled "T_g measured or estimated from T_m". Is the data presented in Figure 3 a further subset of the data in Figs 1 and 2? I suspect they are the same data, but this should be made clear.

Response: In the revised manuscript we add a new subsection 2.1 "Dataset of glass transition temperature" to describe the training and test datasets and the methods deriving the values of T_g, C^0 and T_m. In the training dataset, T_g is measured or otherwise estimated from T_m. C^0 and T_m are estimated from the EPI Suite if they were not available from measurements. For the detailed description, please refer to the response to your comment 3. Figure 3 in the ACPD manuscript has been moved to the Appendix as Fig. B1. You are right that the data presented in this figure are a subset of the data in Fig. 1, which is clarified in the caption of revised Fig. B1. We add the following sentences in the revised manuscript:

Line 553-555: "Figure B1 compares the measured T_g included in the training dataset shown in Fig. 1a to T_g predicted by (a) C^0 and the atomic O:C (Eq. 1), (b) elemental composition (Eqs. A1-A3), and (c) Eq. (B1) by Zhang et al. (2019)".

After reading the manuscript I'm not left with a clear conclusion regarding the utility

of these parameterizations to predict the phase of organics in the atmosphere. As the authors point out, T_g predictions span a range of 100 K depending on how volatility is estimated from the same dataset. The predicted T_g range also unfortunately spans the tropospheric T range, so that the uncertainty is precisely in the temperature range where there is high sensitivity to T_g. It wouldn't matter much if the predicted T_g range was 100-200 K, but that's not the case. The effect of RH makes this even more unclear, with a very wide range of viscosity predicted below 60-70% RH (Fig 7). For example, line 31 states that T_g varies from 290 – 339 K from which I would conclude that OA should exist predominantly in a glassy state under ambient conditions. However, examining Figure 7 leads to a substantially different conclusion. At the end, I wasn't left with much confidence in the ability to predict organic phase, even for a fixed T, RH, and organic aerosol composition. The predicted ranges are exceptionally wide, even before considering uncertainty. I don't have a specific suggested remedy, but I think it is something the authors need to address.

Response: This comment arises from the original Fig. 4 showing that the T_g of total OA under dry conditions is very different (span a range of 100 K as you pointed) predicted by different C^* distributions measured during the SOAS campaign. Note that this wide range stems mostly from variations in measured volatility distributions, but not from uncertainties of our T_g parameterizations and viscosity prediction method. In the ACPD manuscript we have stated that the credible $T_{g,org}$ values span in the range of 313 – 330 K and the predicted low values (< 280 K) estimated from the "Formulas" and "Partitioning" methods in Stark et al. (2017) are not credible. Our parameterizations can reasonably predict the T_g of ambient OA when measured C^* distributions are well constrained. The predicted viscosity of OA in SOAS is consistent with the ambient particle phase state measurements during the SOAS campaign (please see also our response for your comment 5). The T_g varying from 290 – 339 K stated in Line 31 in the abstract is the predicted T_g of total OA at the dry condition ($T_{g,org}$) at the eleven field sites. We clarified this point in the revised abstract. The pink shaded area in Fig. 7 (Fig. 5 in the revised manuscript) bounds the predicted viscosities of MO-OOA and LO-OOA in three different locations, thus the pink shaded area spans wide at medium / low RH, as the $T_{g,org}$ and hygroscopicity of these OA factors at different locations are different (please also refer to our response to your comment 2). We predict the viscosity of the OOA factor as OOA is often considered to represent SOA, and the predicted viscosity of OOA is consistent with the viscosity of SOA formed from various precursors. The above comparison shows the parameterization developed in this study can reasonably predict the phase state of ambient OA as well as laboratory-generated SOA. We add the following sentences in the revised manuscript:

Line 260-263: "Figure 2 shows that $T_{g,org}$ of total OA (TOA) range from 232 K to 334 K, depending on volatility distributions measured by different methods, while the most credible predicted $T_{g,org}$ values span in the range of 313 – 330 K. The reasons are stated below by comparing the different methods deriving the C^* distributions".

Line 303-308: "These analyses indicate that the volatility distributions derived from different methods, even when based on the same measurements, significantly affect the predicted $T_{g,org}$, and the most atmospherically relevant volatility distributions

should be carefully chosen to reasonably predict the glass transition temperature of ambient OA. In summary, the $T_{g,org}$ values during the SOAS campaign should be in the range of 313 – 330 K".

(2) Address the applicability of using a parameterization based on pure compounds to predict properties of mixtures (e.g. SOA).

I second the editor's comment regarding viscosity and T_g of complex mixtures. The authors should address, early in the manuscript, uncertainties in applying a parameterization based on pure compounds to SOA, which is a complex mixture. I don't expect the authors to solve this, but it should be addressed early in the paper.

Response: Following your suggestion, we added a sentence to acknowledge additional uncertainty in the method section. We added a new subsection "2.3 Predictions of T_g and viscosity of organic aerosols" in the Method section. We assumed ideal thermodynamic mixing when applying the T_g parameterization to a certain volatility bin containing multiple components. After the T_g in a certain C^* is known, the T_g of SOA mixtures is calculated by the Gordon-Taylor equation and we state the limitation of the Gordon-Taylor equation in the revised manuscript. We add the following sentences:

Line 205 -208: "Note that there may be additional uncertainty in application of T_g parameterizations (which were developed based on pure compounds) to each volatility bin representing surrogate of complex multicomponent mixtures."

Line 228-233: "The Gordon-Taylor approach has been validated for a wide range of mixtures including SOA compounds (Dette et al., 2014; Lessmeier et al., 2018). The Gordon-Taylor approach may fail in the case of adduct or complex formation (Koop et al., 2011), which is highly unlikely in multicomponent mixtures with myriads of SOA compounds with very small individual mole fractions and thus particular interactions between individual compounds are more likely to average out (Shiraiwa et al., 2017); this aspect would need to be investigated in future studies".

I also second the editors comment on Figure 7 and the discussion of T_g of PMF-derived factors. I'm not sure what it even means to have a predicted viscosity/ T_g of HOA, COA, MO-OOA, etc. since they are always mixed with other factors in the real atmosphere. Again, the authors can't be expected to solve this, but more context in the text is needed early in the manuscript.

Response: We predicted T_g of OA factors as their volatility distributions were available and we think that comparison of T_g of these factors would be useful to compare with measured viscosities of laboratory-generated SOA, given that OOA may correspond to SOA (Jimenez et al., 2009). In the revised manuscript we have shortened the description of T_g of the characterized OA factors and explained the reasons why we compare the viscosity of OOA factors with the viscosity of laboratory-generated SOA. We also added a sentence to note potential limitations of this analysis.

Line 378-382: "Note that these different OA factors may often be internally mixed

in ambient atmosphere and predicted $T_{g,org}$ and particle viscosity would be irrelevant in such a case. Nevertheless, these predictions can be useful when particles are externally mixed or ambient OA are dominated by a certain OA factor".

Line 406-407: "The predicted behavior of BBOA is in line with bounce measurements observing that particles are semisolid in a biomass burning plume (Bateman et al., 2017)".

Line 410-419: "There have been growing measurements of RH-dependent viscosity of laboratory-generated SOA formed from different precursors, e.g., isoprene (Song et al., 2015), α-pinene (Abramson et al., 2013; Renbaum-Wolff et al., 2013; Kidd et al., 2014; Pajunoja et al., 2014; Bateman et al., 2015; Zhang et al., 2015; Grayson et al., 2016; Petters et al., 2019), toluene (Song et al., 2016a) and diesel fuel (Song et al., 2019). As the OOA factors characterized from ambient AMS observations may represent ambient SOA (Jimenez et al., 2009), the predicted viscosities of OOA are compared with laboratory measurements of SOA viscosities in Fig. 5b. It shows that the majority of experimental values is well bounded by the predicted viscosities of OOA, represented by the pink shaded area".

(3) Address the uncertainty/error in the inputs to the parameterizations.

I applaud the authors for making the best possible use of the available data and I understand they are trying to estimate properties of as many compounds as possible. However, I suggest they more thoroughly address errors in the data used to build the parameterizations (aside from applicability issues above) and clarify when inputs are measured vs calculated. The authors provide prediction bounds, but my interpretation is that these are largely related to errors in fitting. What about errors in predicting T_g and C^o? How large are the errors associated with assigning a fixed factor of $T_g = 0.7 * T_m$ for a wide range of compounds? Can the authors compare measurements of T_g to T_g derived from T_m and show that plot in the SI? I browsed through the SI but didn't find reference to measured values of T_g, but surely there must be some measured T_g for pure compounds? How many compounds with both measured T_g and measured $\boldsymbol{C^o}$ are in the training dataset? Are there any? Can the authors provide a plot of measured $\boldsymbol{C^o}$ vs estimated $\boldsymbol{C^o}$ in the SI? Casual perusal suggests estimated $\boldsymbol{C^o}$ can be very far from measured $\boldsymbol{C^o}$, which will in turn introduce error into the T_g prediction. Lines 155-156 mentions that T_m is estimated, but most other references to T_m say it is measured (e.g. line 201). Is T_m calculated or it measured?

Response: In the revised manuscript we add a new subsection to describe the training and test datasets and the methods deriving the values of T_g, C^0 and T_m. The training dataset is used to develop the parameterizations and T_m is measured or otherwise estimated from the EPI Suite. The test dataset is used to validate the parameterizations and all of the T_m values are estimated from the EPI Suite. We have included Table S1 showing the number of compounds with their T_g, C^0 and T_m measured or otherwise estimated. Most CH, CHO, and CHON compounds have measured T_g, C^0 or T_m; relatively large uncertainty in the inputs data exists in CHOS compounds as only 1 CHOS compound has measured T_g (Zhang et al., 2019). To make our parameterizations also applicable to CHOS compounds, we include other CHOS compounds (Li et al.,

2016) with both C^0 and T_m estimated from the EPI Suite. We include Fig. S1 showing (a) the comparison of measured T_g and the T_g estimated by the Boyer–Kauzmann rule and (b) the comparison of C^0 measured and estimated from the EPI suite. We add the following sentences in the revised manuscript to address the uncertainty in our input data:

Line 127-153: "Measured T_g values are available for 42 CH compounds, 259 CHO compounds, 35 CHON compounds and 1 CHOS compound (Koop et al., 2011; Rothfuss and Petters, 2017; Lessmeier et al., 2018; Zhang et al., 2019), among which there are 168 compounds with measured C^0 available (Table S1). When T_g measurements are unavailable, T_g is estimated from the melting temperature (T_m) applying the Boyer-Kauzmann rule of $T_g = g \cdot T_m$ (Kauzmann, 1948; Boyer, 1954) with $g = 0.70085$ (± 0.00375) (Koop et al., 2011), referred to "estimated T_g" in this study (see good agreement of measured and estimated T_g in Fig. S1a). 1187 compounds (391 CH, 537 CHO, 241 CHON and 18 CHOS compounds) with both measured T_m and C^0 (Table S1, S2) are adopted from the MPBPWIN Program Test Sets (http://esc.syrres.com/interkow/EpiSuiteData.htm) included in the Estimation Programs Interface (EPI) Suite software version 4.1 (US EPA, 2015). Measured T_g, T_m or C^0 for CHOS compounds are sparse and we adopt 850 CHOS compounds included in Li et al. (2016) with their T_m and C^0 estimated by the EPI Suite software (Table S2). There are estimation limitations in the EPI Suite; for example, the disagreement between measured and estimated C^0 is larger for compounds with $C^0 < \sim 10^{-2}$ μg m^{-3} (Fig. S1b), which may affect the T_g predictions for compounds with low volatility. However, given the large amount of data points with measured C^0 included in the training dataset, the estimation bias introduced by the EPI Suite may not substantially impact the accuracy of the parameterization developed in this study.

The test dataset used to validate the performance of the parameterizations predicting T_g of SOA components includes 654 CHO compounds and 212 CHON compounds found in SOA oxidation products (Shiraiwa et al., 2014). The values of their C^0 are estimated using the EVAPORATION model (Compernolle et al., 2011). Their T_m values are adopted from the EPI Suite. The T_g predicted by our parameterizations are compared with the T_g estimated from the T_m applying the Boyer-Kauzmann rule in the test dataset".

Table S1. Number of the compounds included in the training dataset and their T_g, C^0 and T_m measured or otherwise estimated.

	CH	CHO	CHON	CHOS
Both T_g and C^0 measured	38	125	5	0
Measured T_g, C^0 estimated from EPI Suite	4	134	30	1
T_g estimated from measured T_m, measured C^0	391	537	241	18
T_g estimated from T_m, T_m estimated from EPI Suite, measured C^0	0	0	0	11
T_g estimated from measured T_m, C^0 estimated from EPI Suite	0	0	0	63
T_g estimated from T_m, T_m and C^0 estimated from	0	0	0	850

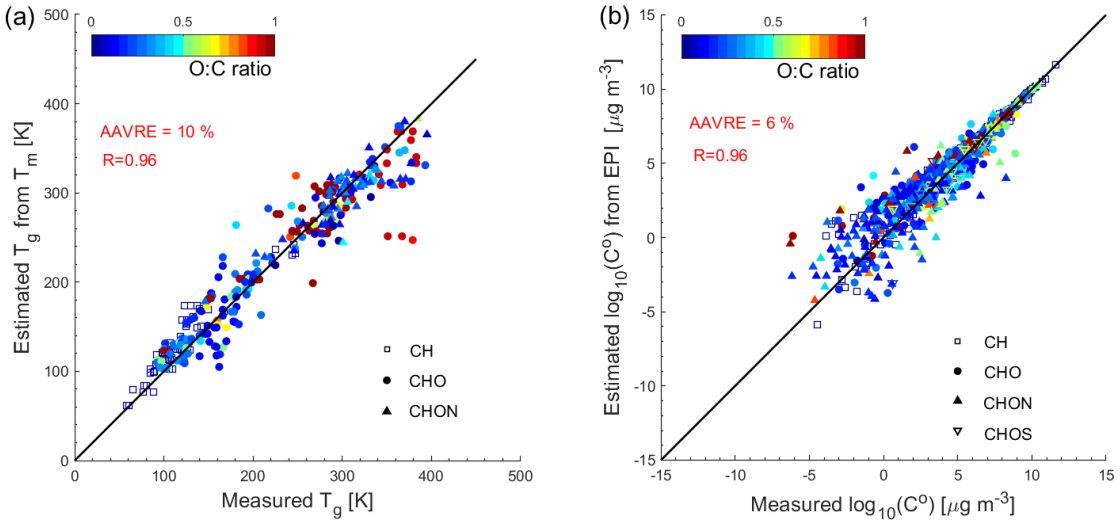

Figure S1. (a) Comparison of the measured T_g (Koop et al., 2011; Dette et al., 2014; Rothfuss and Petters, 2017; Lessmeier et al., 2018; Zhang et al., 2019) and the T_g estimated by the Boyer–Kauzmann rule for 336 organic compounds with their measured T_m available. (b) Comparison of pure compound saturation mass concentration (C^0) measured and estimated from the EPI suite for 1637 organic compounds included in the training dataset in this study.

(4) Lines 286-292. Lines 306-311

Are the volatility distributions derived only for the organic acid portion of the SOA? If so, how would this bias the measurements? Wouldn't organic acids be on the lower end of the volatility distribution, all else being equal? How are the CIMS measurements biased or impacted by the ion chemistry employed? The reference indicates acetate ion chemistry was used and that it is sensitive to acids but not other SOA components. So, wouldn't the thermogram method be biased toward low volatility compounds? The authors indicate that the formulas method is biased by decomposition of SOA. How does the thermogram method deal with decomposition products, which are indicated to be extensive?

Response: It is correct that acetate CIMS mainly measures organic acids, besides a few other compounds such as phenols and other compounds with acidic hydrogen. While this indeed somewhat biases the measurements, the acid fraction in SOA has been shown to be high, as pointed out in the manuscript and referenced (Yatavelli et al., 2015). Further, we disagree that organic acids populate a particularly low volatility region since they show a broad range of O:C and carbon number range, similar to other SOA components such as alcohols, aldehydes, ketones, peroxides, etc. Lastly, the thermogram method certainly includes thermograms of species thermally decomposing rather than desorbing from the filters. However, the peak temperatures of these thermograms relate to volatilities closer to the species volatility than from the other methods and can therefore still be seen as better overall volatility measurements than the other two methods. We have added an extra sentence as below:

Line 272-275: "While this method may be influenced by thermal decomposition, the peak temperatures of decomposing species can be expected to relate closer to actual volatilities than any of the other two analysis methods (Stark et al., 2017)".

(5) Lines 331 and subsequent discussion on RH.

It wasn't very clear how the T_g parameterization presented earlier in the paper relate to the calculations of RH effects. Is the T_g parameterization used in the calculation of T_g of the water/organic mixtures or are these calculations independent of each other? Can the authors show the equation for calculating T_g of water/organic mixtures, since this is central to the paper? I found the transition between the bulk of the paper, which focuses on parameterizations of T_g as a function of volatility, to this section of the paper on the impact of RH somewhat abrupt. Can the authors comment on which effect (condensed phase water vs volatility) has a larger influence on organic phase state? For example, at line 321 the authors state that T_g was 313-330 K during SOAS, which would mean the aerosols are primarily in a glassy state. However, on lines 351- 352 they state that the particles were mostly liquids.

Response: The T_g parameterization is used in the calculation of T_g of the water/organic mixtures. In the revised manuscript we describe the procedures calculating the T_g of water/organic mixtures and the viscosity at different T and RH in the new subsection 2.3 "Predictions of T_g and viscosity of organic aerosols". We added one sentence at the beginning of this paragraph to explain why we further predict the viscosity at given RH to prevent an abrupt transition between sections. The $T_{g,org}$ was predicted to be 313-330 K during the SOAS campaign, indicating that OA are primarily in a glassy state at the dry condition. To compare with the ambient phase state measurements, we calculate the viscosity at different RH and the average T during SOAS. The predicted viscosity is liquid at RH of 83 % and semi-solid at RH of 50 %, consistent with the particle bounce measurements. We add a few sentences in the revised manuscript discussing the influence of condensed phase water vs volatility on phase state.

Lines 235-249: "Under humid conditions, the water content in OA can be estimated using the effective hygroscopicity parameter (κ) (Petters and Kreidenweis, 2007). The T_g of organic-water mixtures ($T_g(w_{org})$) at given RH can be estimated using the Gordon-Taylor equation (Gordon and Taylor, 1952):

$$T_g(w_{org}) = \frac{(1-w_{org})T_{g,w}+\frac{1}{k_{GT}}w_{org}T_{g,org}}{(1-w_{org})+\frac{1}{k_{GT}}w_{org}} \quad (6)$$

where w_{org} is the mass fraction of organics in particles; $T_{g,w}$ is the glass transition temperature of pure water (136 K, Kohl et al., 2005), and k_{GT} is the Gordon-Taylor constant for organic-water mixtures which is suggested to be 2.5 (Zobrist et al., 2008; Koop et al., 2011). Viscosity can then be calculated applying the Vogel-Tammann-Fulcher (VTF) equation (Angell, 1991): $\eta = \eta_\infty e^{\frac{T_0 D}{T-T_0}}$, where η_∞ is the viscosity at infinite temperature (10^{-5} Pa s, Angell, 1991), D is the fragility parameter which is assumed to be 10 (DeRieux and Li et al., 2018), and T_0 is the Vogel temperature calculated as $T_0 = \frac{39.17\,T_g}{D+39.17}$".

Line 318-320: "We further calculate the viscosity of OA based on the $T_{g,org}$ of TOA predicted above in order to compare with the ambient phase state measurements during the SOAS campaign".

Line 337-342: "The variations (313 – 330 K) in $T_{g,org}$ due to the different measured C^* distributions (Fig. 2) have a more significant impact on the predicted viscosity at low and medium RH (Fig. 3a). When RH is higher than ~70 %, the predicted viscosities calculated from different $T_{g,org}$ values are very close; at high RH the condensed phase water has a larger influence on the phase state than the volatility does, depending on the hygroscopicity of organic aerosols".

Minor Comments and Technical Corrections

General comment. There are quite a few typos and grammatical errors through the manuscript. This doesn't get in the way of understanding the paper, but it was noticeable. I started to make specific suggestions below but stopped after a few pages of text. A thorough editing would improve the paper.

Response: Thanks for reading our manuscript carefully and the specific suggestions. We have done a thorough editing.

Line 38. I think you mean SOA derived from diesel fuel rather than the viscosity of diesel fuel itself.

Response: Right. The "of" in front of diesel fuel has been deleted.

Line 62. Suggest changing "depending on" to "as a function of". The message of this sentence is unclear, given you cite many measurements of particle phase via particle bounce.

Response: "depending on temperature (T), relative humidity (RH), and chemical composition" has been moved to Line 60.

Line 66. I think you mean "in the bulk organic phase" rather than "bulk organic molecules".

Response: The sentence has been changed to "bulk diffusivity of organic molecules".

Line 72. Add "The" before "Chemical"

Response: Added.

Line 75. Add "a" before "phase"

Response: Added.

Line 113-114. Isn't it more accurate to say that you parameterized the relationship between T_m and C^o? As far as I can tell the vast majority of T_g values are estimated from measured T_m.

Response: The object of this study is to develop parameterizations predicting T_g and further predict the viscosity of ambient organic aerosols. T_g values estimated from T_m are used as part of our training dataset to develop the parameterization for T_g as a

function of C^o. The parameterizations perform well predicting T_g of individual organic compounds (Fig. 1), the viscosity of ambient OA (Fig. 3) and laboratory generated OA (Fig. 5), indicating that estimated T_g values from T_m used in the training dataset would not impact predictions of T_g by the parameterizations developed in this study. Please also refer to our response to your comment 3.

Line 123 add "or" after "measured"
Response: Added.

Line 129. Can the authors state the fraction of the compounds with measured C^o and measured T_g as opposed to estimated values?
Response: The fractions of the compounds with measured C^o and measured T_g as opposed to estimated values in the training dataset are different for different classes (CH, CHO, CHON and CHOS). We have included Table S1 showing the number of compounds with their T_g, C^0 and T_m measured or otherwise estimated. Please see our response to your comment 3.

Line 132. The weak dependence of T_g on O:C is not very clear from Fig. 1a. Suggest graphing this separately, perhaps in the SI.
Response: The dependence of T_g on O:C is included in the SI in the revised manuscript:

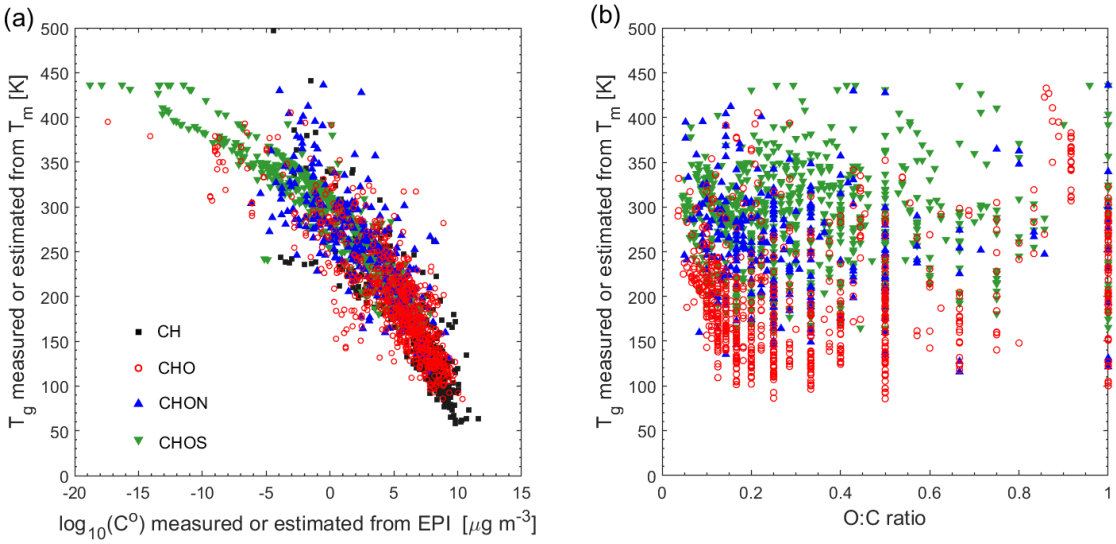

Figure S2. T_g of organic compounds in the training dataset plotted against (a) pure compound saturation mass concentration (C^0) and (b) the atomic O:C ratio.

Lines 155-156. Are T_m values themselves estimate or taken from a database of measured compound melting points?
Response: There are two datasets used in this study. The training dataset is used to develop the parameterizations and T_m is measured or otherwise estimated from the EPI Suite. The test dataset is used to validate the parameterizations and T_m values are all estimated from the EPI Suite. Please also refer to our response to your comment 3.

Line 252 change comparing to compared

Response: Changed.

Lines 289 – 295. It isn't clear how to reconcile 50% of the total OA being composed of organic acids (L289) if "many of the detected species are decomposition products (L294-295)". Please clarify.

Response: The FIGAERO measurement are not used to determine the overall OA composition or, for that matter, the contribution of organic acids to total OA. The 50% value was taken from a separate study, where acetate CIMS measurements were compared quantitatively to AMS measurements (Yatavelli et al., 2015).

We clarified at Line 265: …organic acids (which were shown to account for about half of the total OA; Yatavelli et al., 2015) from…

Lines 292-294. How did the authors convert from the molecular formulas measured by the MS to molecular structure needed for the group contribution methods?

Responses: The details of this algorithm are described in Stark et al. (2017). Briefly, at least one carboxylic acid group was assumed to be present in each formula, while the remaining oxygen was either assumed to be carbonyl, hydroxyl, or carboxyl. The resulting volatility distributions from these three different possibilities were considered in the Stark et al. (2017) paper, but all showed similar distributions in that the volatilities were all very high. In this study, we used the results from the assumption that all remaining oxygen was present in hydroxyl groups, resulting in the lowest volatilities of the possible formula method results. We added a sentence describing a few more details:

Line 272-275: "While this method may be influenced by thermal decomposition, the peak temperatures of decomposing species can be expected to relate closer to actual volatilities than any of the other two analysis methods (Stark et al., 2017)".

Lines 387-389. I can imagine that the aerosol organic loading in Beijing is also significantly larger than at most other sites, which will impact volatility and T_g due to partitioning. Please comment.

Responses: Following your suggestion, we add the following sentence:

Line 385-387: "This may be due to the higher total OA mass concentrations in Beijing (Xu et al., 2019), which facilitates greater partitioning of SVOC compounds into the particle phase, leading to a lower $T_{g,org}$".

Lines 459-461. The particles were solid-like when anthropogenic influence from the Manaus plume dominated.

Response: We revised this sentence at Line 460:

"……while with the anthropogenic influence including both urban pollution and biomass burning, they occur as semi-solid or glassy (Bateman et al., 2016; Bateman et al., 2017)".

Lines 474-477. This is true, but other studies measured or implied kinetic limitations at moderate or high RH. These studies should also be cited.

Response: This sentence has been revised as:

Line 485-489: “Some chamber experiments probing the mixing timescales of SOA particles formed from isoprene, α-pinene, and limonene did not observe significant kinetic limitations at moderate and high RH under room temperature (Loza et al., 2013; Ye et al., 2016), while kinetic limitations of bulk diffusion of organic molecules in β-caryophyllene SOA have been observed at 75 % RH (Ye et al., 2018), warranting further investigations on the degree of kinetic limitations in ambient tropospheric conditions”.

Figures 1-3. Isn’t possible to differentiate among the symbol shapes.
Response: The size of the symbols has been enlarged and the resolution of the figures has been improved.

Figure 1a. Can the fit from equations 1 and 2 be drawn on this figure?
Response: The fit from Eq. 1 and 2 has been added in Fig.1a and Fig. S3a, respectively. We add the following sentences in the Line 171-174:
“The predicted T_g by Eq. (1) is plotted in Fig. 1a with the O:C ratios of 0, 0.5, and 1, showing that the predicted dependence of T_g on C^0 follows the trend well in the training dataset. The O:C ratio mainly affects the predicted T_g of volatile or extremely low volatile compounds”.

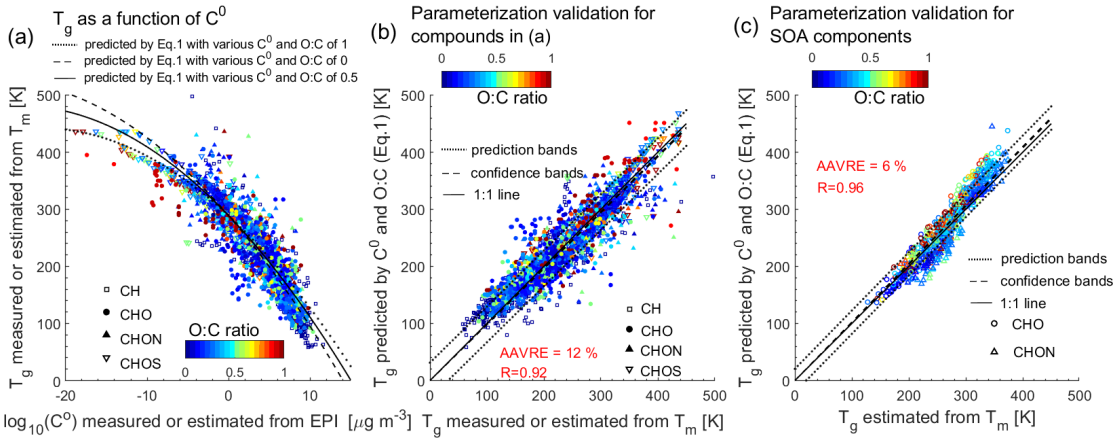

Figure 1. (a) T_g of organic compounds in the training dataset plotted against C^0. The lines show the predictions of T_g (Eq. 1) by C^0 and the O:C ratio of 0 (dashed), 0.5 (solid), and 1 (dotted). (b) Predicted T_g by C^0 and the O:C ratio (Eq. 1) for compounds shown in (a) compared to measured or otherwise estimated T_g from T_m. (c) Predicted T_g for SOA components (Shiraiwa et al., 2014) using Eq. (1) plotted against estimated T_g from T_m with the Boyer-Kauzmann rule. The correlation coefficient (R) and the average absolute value of the relative error (AAVRE) are shown. The dashed and dotted lines in (b) and (c) show 68% confidence and prediction bands, respectively.

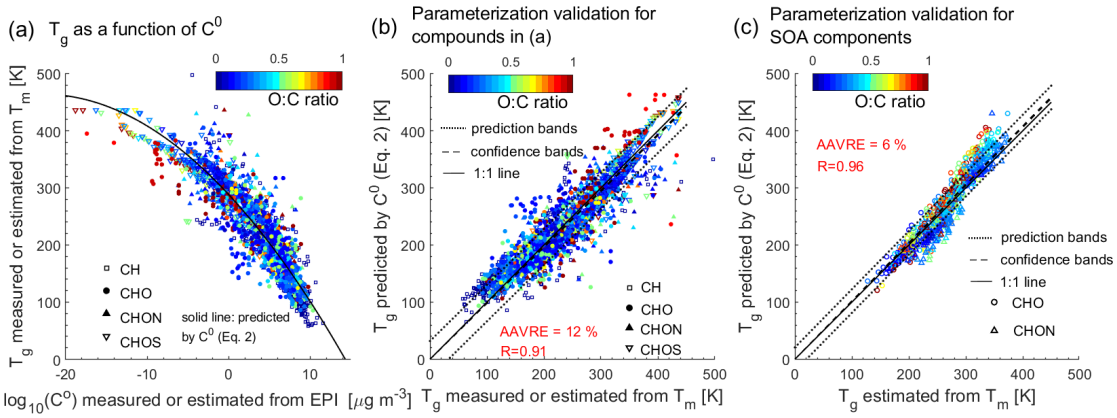

Figure S3. (a) T_g of organic compounds in the training dataset plotted against C^0. The solid line shows the predictions of T_g by C^0 (Eq. 2). (b) Predicted T_g by C^0 (Eq. 2) for compounds shown in (a) compared to measured or otherwise estimated T_g from T_m. (c) Predicted T_g for SOA components (Shiraiwa et al., 2014) using Eq. (2) plotted against estimated T_g from T_m with the Boyer-Kauzmann rule. The correlation coefficient (R) and the average absolute value of the relative error (AAVRE) are shown. The dashed and dotted lines in (b) and (c) show 68% confidence and prediction bands, respectively.

Figure 3. Clarify whether Measured T_g is the same as T_g estimated from T_m as in Figures 1 and 2.

Response: The comparison between the measured T_g and the T_g estimated from T_m has been shown in Fig. S1. Please refer to our response to your comment 3. The original Figure 3 has been moved to the Appendix B and revised clarifying the measured T_g are the same as the measured T_g shown in Fig. 1a.

Figure 4 caption. It isn't clear what "edge lines are in grey" refers to.

Response: It has been changed to "marker edge lines are in grey".

Response to the comments of Anonymous Referee #2

Referee General Comment: The manuscript by Li et al. extends the previous parameterizations of the glass transition temperature (T_g) based on the vapor pressure of a large number of pure organic compounds. The authors explore several parameterizations and use them to estimate ambient organic aerosol viscosity. The diversity of parameterizations is useful but can be distracting form the take-home message of the manuscript. After revisions of the modeling description and discussion section, this manuscript should be published. On the content of the manuscript, the main points I take away are the new parameterizations and their modeling of ambient data. Some of the details presented deviate from this main narrative (i.e., multiple FIGAERO-CIMS analysis), so even though the details may be necessary for the calculations, they distract from the narrative. I would suggest putting details that are not key to manuscript narrative into the supplemental information, which will help improve the message of the manuscript.

Response: We thank Referee #2 for the review and the positive evaluation of our manuscript. To improve the presentation quality, we divide the Method section into three subsections and keep the main parameterization predicting the glass transition temperature as a function of volatility in the main text. We move other parameterizations and related comparisons to the Appendix to focus the narrative of the manuscript.

Referee Major Specific Comment:

1. Parameterizations section: This section needs subsections to delineate the different models. Also tell the reader which of these parameterizations is most important to focus on for the rest of the paper. Or you could add an introduction paragraph to this section, where you discuss the merits of each model parameterizations. A revision along those lines would help focus the narrative of the manuscript.

Response: In the revised manuscript we move the parameterizations predicting T_g as a function of elemental compositions to Appendix A; the comparison of T_g predictions with Zhang et al. (2019) to Appendix B. We divide the Method section into three subsections as below:

"2.1 Dataset of glass transition temperature"

Section 2.1 describes the training dataset used to develop parameterizations and the test dataset used to validate the parameterizations predicting T_g of SOA components. This section also addresses the uncertainty in the input data. Please refer to our responses to the comment 3 from the Referee 1.

"2.2 Parameterizations of T_g as a function of volatility"

"2.3 Predictions of T_g and viscosity of organic aerosols"

2. Figure 1-3: These Figures do not stand apart very well, and conceptually blur. If you delineate the parameterizations more, that will help in understanding the importance of each Figure. To me, Figures 1b and 1c convey similar information (i.e., good predictive behavior), so show one and put the other in the SI. The O:C ratio coloring could be removed (since the lack of correlation could just be stated in the text) and instead color

by functional group. Figure 3 could be replaced in a table that summarizes the AAVRE and R-squared values.

Response: The resolution of the figures has been improved. We keep both Fig. 1b and 1c in the main text as the dataset in Fig. 1b is same as the points in Fig. 1a, which were used to develop the parameterizations (training dataset). The points in Fig. 1c were used as the test dataset to validate the performance of the parameterizations predicting T_g of SOA components. In the revised manuscript we add a new subsection 2.1 describing the training dataset and the test dataset. Please also refer to our response to the comment 3 of Referee 1. We keep the markers in Fig.1 color-coded by the O:C ratio. We add the following sentences in the revised main text to state the reason:

Line 160-162: "Note that a tight correlation between T_g and the O:C ratio has been observed for oxidation products formed from specific precursors including α-pinene (Dette et al., 2014), *n*-heptadecane and naphthalene (Saukko et al., 2012)".

Following your suggestion, we added Fig. S2a showing the dependence of T_g on C^0 with markers color-coded by chemical composition:

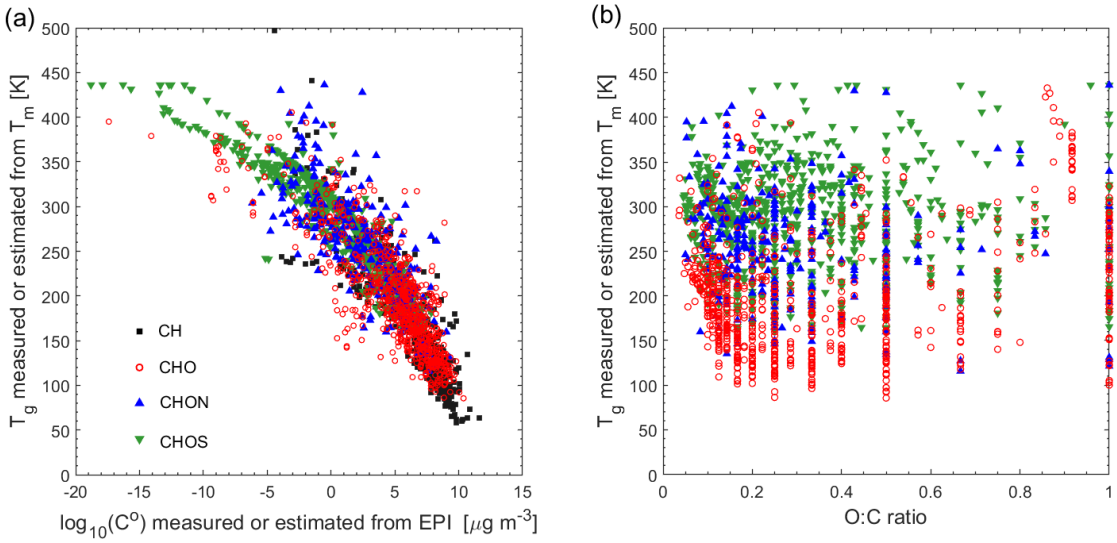

Figure S2. T_g of organic compounds in the training dataset plotted against (a) pure compound saturation mass concentration (C^0) and (b) the atomic O:C ratio.

We move the Fig. 3 in the ACPD to the Appendix B. We keep this figure as it is necessary to show the comparison of our parameterizations with the parameterization in Zhang et al. who also related T_g to volatility (they used the vapor pressure instead of the saturation mass concentration).

3. Field Observations: Line 259: I suggest adding a sentence motivating why Figure 4 is shown and what the reader will gain from it. I take away that viscosity can be estimated from C^* measurements and ambient OA spans solid to liquid states depending on the method used, was that the main message?

Response: Yes, correct. We have added the following sentence:

Line 253-255: "In this section we predict glass transition temperatures and phase state of ambient OA during the SOAS campaign which took place in the southeastern

United States (Centreville, Alabama) in summer 2013 (Carlton et al., 2018)".

4. Line 286: The discussion of the FIGAERO-CIMS analysis can be shortened, as the main point starts at Line 312.

Responses: We re-arrange this paragraph by stating the main point at the beginning, moving the less credible $T_{g,org}$ values calculated from the "Formulas" and "Partitioning" methods to another paragraph:

Lines 260-263: "Figure 2 shows that $T_{g,org}$ of total OA (TOA) range from 232 K to 334 K, depending on volatility distributions measured by different methods, while the most credible predicted $T_{g,org}$ values span in the range of 313 – 330 K. The reasons are stated below by comparing the different methods deriving the C^* distributions".

Lines 283-285: "The lower $T_{g,org}$ values (< 280 K) calculated from the C^* distributions estimated from the "Formulas" and "Partitioning" methods (Stark et al., 2017) are less atmospherically relevant".

Lines 303-308: "These analyses indicate that the volatility distributions derived from different methods, even when based on the same measurements, significantly affect the predicted $T_{g,org}$, and the most atmospherically relevant volatility distributions should be carefully chosen to reasonably predict the glass transition temperature of ambient OA. In summary, the $T_{g,org}$ values during the SOAS campaign should be in the range of 313 – 330 K".

5. The added value of Figure 8 seems to be limited. If the goal is to show how well the CTM model output and your T_g models agree, this is not the ideal way to show that. It would be clearer to pull the viscosity values for each of the 11 sites from the CTM output and make a scatter plot vs. the measurement derived viscosities. The actual global distributions are irrelevant for this comparison, and instead, point the reader to the Shiraiwa et al. (2017) paper.

Response: Following your suggestion, we have added the scatter plot (Fig. 6b in the revised manuscript). We keep the global distributions as Fig. 6a, as global distributions of viscosity are new and were not included in Shiraiwa et al. (2017). We edited the main text as follows:

Line 449-452: "the amorphous solid or semi-solid phase occurs over relatively dry areas, including the sites in western US, Mexico City, Beijing and coastal sites in Greece; the lower viscosity occurs in southeastern US and Paris".

Line 464-467: "Similar cases are observed in Athens and the two sites in the western US, that our predictions based on volatility distributions indicate the glassy phase state while the global model predicts the occurrence of a semi-solid phase".

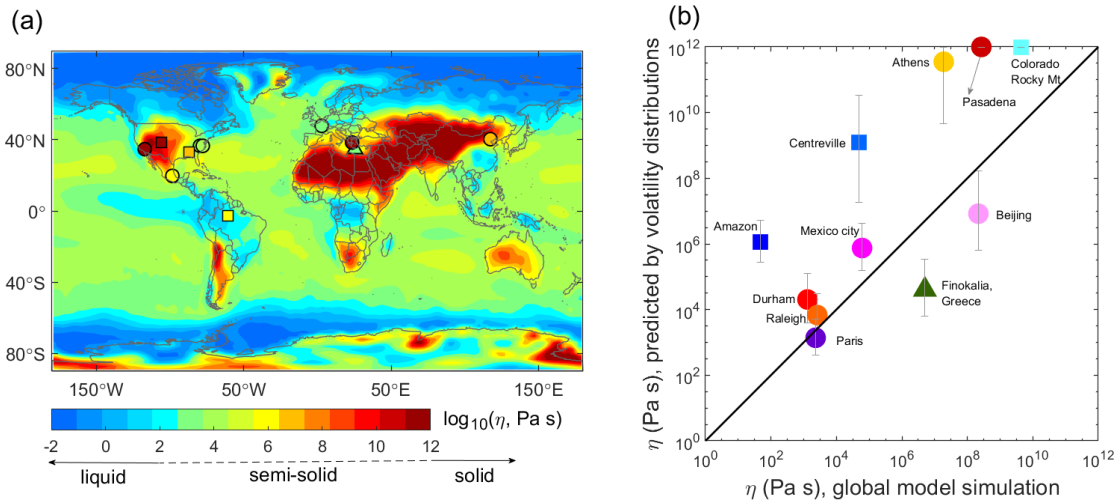

Figure 6. (a) Global distributions of SOA annually averaged viscosity at the surface simulated by a global chemical transport model (Shiraiwa et al., 2017) with the viscosity predicted by measured volatility distributions at 11 global sites (triangle, square and circle represent remote, forested and urban sites, respectively, Table S3). The color code indicates viscosity in a log scale. (b) Predicted viscosity based on measured volatility distributions compared against the viscosity in global simulations. The error bars correspond to uncertainties in viscosities calculated from uncertainties in predicted $T_{g,org}$ shown in Fig. 4.

6. Conclusion/discussion: I think a short conclusion or discussion would help tie the previous treatise of field observations and put them in a broader context. This is already started at Line 477 and should be expanded on.

Responses: We have put conclusions and implications in the new Section 5:

"**5. Conclusions and implications**

We have developed parameterizations to estimate the glass transition temperature of organic compounds using saturation mass concentration (C^0) and atomic O:C ratio. They can be applied to ambient observations of volatility distributions to estimate viscosity of ambient organic aerosols. The T_g and viscosity prediction method can be applied in the volatility basis set or the molecular corridor-based approach to improve OA simulations in chemical transport models by consideration of effects of particle viscosity on OA formation and evolution (Shiraiwa et al., 2017; Pye et al., 2017; Schmedding et al., 2019). Most of the current chemical transport models treat particles as homogeneously well-mixed liquid without considering particle-phase diffusion limitations, which can lead to bias in simulations of SOA mass concentrations and evolution of size distributions (Shiraiwa and Seinfeld, 2012; Zaveri et al., 2018). The SOA simulations applying the VBS framework have not yet included the effects of viscosity on SOA formation and evolution. When the gas-particle partitioning is limited by bulk diffusion, kinetic treatments of SOA partitioning may need to be applied (Perraud et al., 2012; Liu et al., 2016; Yli-Juuti et al., 2017; Li and Shiraiwa, 2019). Some chamber experiments probing the mixing timescales of SOA particles formed from isoprene, α-pinene, and limonene did not observe significant kinetic limitations at

moderate and high RH under room temperature (Loza et al., 2013; Ye et al., 2016), while kinetic limitations of bulk diffusion of organic molecules in β-caryophyllene SOA have been observed at 75 % RH (Ye et al., 2018), warranting further investigations on the degree of kinetic limitations in ambient tropospheric conditions. In addition, the interplay of diffusion limitations and phase separation impacts heterogeneous and multiphase chemistry (Vander Wall et al., 2018; DeRieux et al., 2019; Zhou et al., 2019) and gas-particle partitioning (Zuend and Seinfeld, 2012; Shiraiwa et al., 2013; Freedman, 2017; Pye et al., 2017; Gorkowski et al., 2019a). The particle morphology and the degree of non-ideal mixing and liquid-liquid phase separation can evolve upon atmospheric aging (Gorkowski et al., 2019b). These aspects may also need to be considered for better representation of organic aerosols in future studies".

Line Comments:

1. Line 259: I would stray away from starting a sentence with a variable, as doing so reduces readability (and this paragraph does it repeatedly). So it would change to, "The T_g of ambient..." and line 262, "These T_g values are then placed..."

Response: Thanks for the suggestion. We revised all the sentences which had started with a variable all through the manuscript.

2. Figure 6a: I suggest filling in the dots, with the edge color (TOA, OOA, ...). The T_g fill color is already represented by the contour lines.

Response: We would like to keep the edge color denoting OA factors as the T_g values represented by the contour lines were calculated from the C^* (x-axis) and O:C (y-axis) values in the 2-D VBS framework, which are different from the $T_{g,org}$ values filling the dots calculated from the measured ambient volatility distributions. We clarified this in the caption of Fig. 4a in the revised manuscript:

"The isopleths in (a) correspond to the T_g calculated using Eq. (1) with C^* and O:C defined in the 2D-VBS".

3. Figure 6b: You have already shown the correlation between T_g and C^* (Figure 1a), so the added value to the manuscript is small. I suggest moving Figure 6b to the SI.

Responses: Figure 1a is for individual organic compounds. The correlation between predicted $T_{g,org}$ and the average volatility of ambient OA shown in Figure 6b agrees with the trend shown in Fig. 1a, which indicates that our newly developed parameterization works for ambient OA mixtures.

4. Figure 7 caption: Define BBOA, LO-OOA, and MO-OOA. I didn't find the definitions in the main text.

Responses: These OA factors are now defined in Line 374-378:

"The marker edge color represents OA components identified via source apportionment techniques on AMS mass spectra (Lanz et al., 2007), including biomass burning OA (BBOA), hydrocarbon-like OA (HOA), cooking OA (COA) and oxygenated OA (OOA) which is sometimes further separated into more oxygenated (MO-OOA) and less oxygenated OA (LO-OOA) factors".

Predictions of the glass transition temperature and viscosity of organic aerosols from volatility distributions

Ying Li[1,*], Douglas A. Day[2,3], Harald Stark[2,3,4], Jose L. Jimenez[2,3] and Manabu Shiraiwa[1,*]

[1] Department of Chemistry, University of California, Irvine, CA 92697-2025, USA
[2] Cooperative Institute for Research in Environmental Sciences (CIRES), University of Colorado, Boulder, CO 80309, USA
[3] Department of Chemistry, University of Colorado, Boulder, CO 80309, USA
[4] Aerodyne Research Inc., Billerica, Massachusetts 01821, USA

*Correspondence to: Ying Li (yingl47@uci.edu) or Manabu Shiraiwa (m.shiraiwa@uci.edu)

Abstract:

Volatility and viscosity are important properties of organic aerosols (OA), affecting aerosol processes such as formation, evolution and partitioning of OA. Volatility distributions of ambient OA particles have often been measured, while viscosity measurements are scarce. We have previously developed a method to estimate the glass transition temperature (T_g) of an organic compound containing carbon, hydrogen, and oxygen. Based on analysis of over 2400 organic compounds including oxygenated organic compounds as well as nitrogen- and sulfur-containing organic compounds, we extend this method to include nitrogen- and sulfur-containing compounds based on elemental composition. In addition, parameterizations are developed to predict T_g as a function of volatility and the atomic oxygen-to-carbon ratio based on a negative correlation between T_g and volatility. This prediction method of T_g is applied to ambient observations of volatility distributions at eleven field sites. The predicted T_g of OA under dry conditions vary mainly from 290 K to 339 K and the predicted viscosities are consistent with the results of ambient particle phase state measurements in the southeastern US and the Amazonian rain forest. Reducing the uncertainties in measured volatility distributions would improve predictions of viscosity especially at low relative humidity. We also predict the T_g of OA components identified via positive matrix factorization of aerosol mass spectrometer data. The predicted viscosity of oxidized OA is consistent with previously reported viscosity of SOA derived from α-pinene, toluene, isoprene epoxydiol (IEPOX), and diesel fuel. Comparison of the predicted viscosity based on the observed volatility distributions with the viscosity simulated by a chemical transport model implies that missing low volatility compounds in a global model can lead to underestimation of OA viscosity at some sites. The relation between volatility and viscosity can be applied in the molecular corridor or volatility basis set approaches to improve OA simulations in chemical transport models by consideration of effects of particle viscosity in OA formation and evolution.

1. Introduction

Organic aerosols (OA) contribute substantially to the mass loadings of atmospheric fine particulate matter (Hallquist et al., 2009; Jimenez et al., 2009). OA formed from various anthropogenic or biogenic precursors have complex physicochemical properties (Goldstein and Galbally, 2007; Nizkorodov et al., 2011; Ditto et al., 2018), which makes predictions of their role in air quality, climate and public health challenging (Kanakidou et al., 2005; Shrivastava et al., 2017). Volatility and viscosity are important properties of OA, both of which affect important aerosol processes such as gas–particle partitioning, new particle formation and evolution of size distribution, heterogeneous reactions, and cloud condensation and ice nucleation pathways of OA, as summarized in recent review articles (Krieger et al., 2012; Bilde et al., 2015; Pöschl and Shiraiwa, 2015; Knopf et al., 2018; Reid et al., 2018).

Recent measurements have shown that OA can exist in liquid (low dynamic viscosity η; $\eta < 10^2$ Pa s), semi-solid ($10^2 \leq \eta \leq 10^{12}$ Pa s), and amorphous solid ($\eta > 10^{12}$ Pa s) states, depending on temperature (T), relative humidity (RH), and chemical composition (Reid et al., 2018). Even though there are several particle bounce measurements to infer ambient OA phase state, there are limited ambient measurements of particle phase state or viscosity (Virtanen et al., 2010; O'Brien et al., 2014; Bateman et al., 2016; Pajunoja et al., 2016; Bateman et al., 2017; Liu et al., 2017; Ditto et al., 2019; Slade et al., 2019). Viscosity can be directly converted to bulk diffusivity of organic molecules using the Stokes–Einstein equation, which has been shown to work well for organic molecules diffusing through low viscous materials (Price et al., 2016; Chenyakin et al., 2017). This relation is inapplicable for predicting the bulk diffusivity of water and small molecules and it may also underestimate the diffusivity of organic molecules in a highly viscous matrix, which can be corrected using a fractional Stokes-Einstein equation (Price et al., 2016; Evoy et al., 2019).

Viscosity can be related to the glass transition temperature (T_g), at which a phase transition between amorphous solid and semi-solid states occurs (Koop et al.,

2011). Ambient temperature varies through 100 K throughout the troposphere, greatly influencing the viscosity of the mixture. When the ambient temperature is below T_g, an amorphous particle behaves as a solid, while a particle would be semi-solid or liquid when the ambient temperature is above T_g. OA particles contain a number of organic compounds and also a variable amount of liquid water depending on RH, which can act as a plasticizer to reduce T_g: these mixture effects can be estimated using the Gordon-Taylor relation (Mikhailov et al., 2009; Koop et al., 2011; Dette et al., 2014). In addition, ambient OA may often be internally mixed with inorganic species such as sulfate and nitrate, which would further lower T_g and viscosity if they are well-mixed in one phase; when the phase separation occurs, the inorganic-rich and organic-rich phases may undergo glass transition at different temperatures (Dette and Koop, 2015).

For pure organic compounds with known molecular structure, viscosity can be predicted by group contribution approaches (Cao et al., 1993; Bosse, 2005; Song et al., 2016b; Rovelli et al., 2019; Gervasi et al., 2020); chemical composition of ambient OA is complex and molecular specificity is often unavailable, which makes viscosity predictions of ambient OA challenging. We have recently developed a set of semi-empirical parameterizations using molar mass (M) and atomic O:C ratio (Shiraiwa and Li et al., 2017) or elemental composition (DeRieux and Li et al., 2018) to predict T_g for compounds comprised of carbon, hydrogen, and oxygen (CHO compounds). These parameterizations have been applied to high-resolution mass spectrometry measurements to estimate viscosity of organic aerosols (DeRieux and Li et al., 2018; Schum et al., 2018; Ditto et al., 2019; Song et al., 2019) and coupled into a thermodynamic model (Gervasi et al., 2020). Note that heteroatoms and the effects of molecular structure and functional groups on T_g are not considered in parameterizations of Shiraiwa and Li et al. (2017) and DeRieux and Li et al. (2018).

Viscosity of pure compounds has been found to be inversely correlated with vapor pressure (Thomas et al., 1979). The molecular corridor (Shiraiwa et al., 2014; Li et al., 2016) based analysis of hundreds of SOA components has shown that compounds

with lower pure compound saturation mass concentration (C^0) have higher T_g (Shiraiwa et al., 2017). Rothfuss & Petters (2017) found that there is a similar trend between the sensitivity of viscosity to functional group addition and the sensitivity of vapor pressure to functional group addition. Measurements of the evaporation kinetics of maleic acid showed that decreasing particle viscosity leads to a suppression in the effective vapor pressure of maleic acid (Marshall et al., 2018). Champion et al. (2019) found secondary organic aerosols (SOA) with higher condensed-phase fractions of extremely low (ELVOC) and low volatile organic compounds (LVOC) showed an increased viscosity. Zhang et al. (2019) measured T_g of isoprene SOA components including isoprene hydroxy hydroperoxide (ISOPOOH), isoprene-derived epoxydiols (IEPOX), 2-methyltetrols, and 2-methyltetrol sulfates (2-MT-OS), observing a tight correlation between T_g and vapor pressure.

Based on the above evidence showing a close relation between volatility and viscosity, in this study we develop the parameterizations predicting T_g as a function of C^0 based on data from over 2000 compounds. Functional group contribution approaches are often used to predict C^0 (Capouet and Müller, 2006; Pankow and Asher, 2008; Compernolle et al., 2011; O'Meara et al., 2014), thereby using C^0 to predict T_g would include the molecular structure effect indirectly. The developed parameterizations are applied to field observations of volatility distributions to predict viscosity of ambient OA.

2. Methods

2.1 Dataset of glass transition temperature

The training dataset used to develop the parameterizations of T_g include 2448 organic compounds classified into four classes (see the number of CH, CHO, CHON, and CHOS compounds in Table S1). Measured T_g values are available for 42 CH compounds, 259 CHO compounds, 35 CHON compounds and 1 CHOS compound (Koop et al., 2011; Rothfuss and Petters, 2017; Lessmeier et al., 2018; Zhang et al.,

2019), among which there are 168 compounds with measured C^0 available (Table S1). When T_g measurements are unavailable, T_g is estimated from the melting temperature (T_m) applying the Boyer-Kauzmann rule of $T_g = g \cdot T_m$ (Kauzmann, 1948; Boyer, 1954) with $g = 0.70085$ (±0.00375) (Koop et al., 2011), referred to "estimated T_g" in this study (see good agreement of measured and estimated T_g in Fig. S1a). 1187 compounds (391 CH, 537 CHO, 241 CHON and 18 CHOS compounds) with both measured T_m and C^0 (Table S1, S2) are adopted from the MPBPWIN Program Test Sets (http://esc.syrres.com/interkow/EpiSuiteData.htm) included in the Estimation Programs Interface (EPI) Suite software version 4.1 (US EPA, 2015). Measured T_g, T_m or C^0 for CHOS compounds are sparse and we adopt 850 CHOS compounds included in Li et al. (2016) with their T_m and C^0 estimated by the EPI Suite software (Table S2). There are estimation limitations in the EPI Suite; for example, the disagreement between measured and estimated C^0 is larger for compounds with $C^0 < \sim 10^{-2}$ μg m^{-3} (Fig. S1b), which may affect the T_g predictions for compounds with low volatility. However, given the large amount of data points with measured C^0 included in the training dataset, the estimation bias introduced by the EPI Suite may not substantially impact the accuracy of the parameterization developed in this study.

The test dataset used to validate the performance of the parameterizations predicting T_g of SOA components includes 654 CHO compounds and 212 CHON compounds found in SOA oxidation products (Shiraiwa et al., 2014). The values of their C^0 are estimated using the EVAPORATION model (Compernolle et al., 2011). Their T_m values are adopted from the EPI Suite. The T_g predicted by our parameterizations are compared with the T_g estimated from the T_m applying the Boyer-Kauzmann rule in the test dataset.

2.2 Parameterizations of T_g as a function of volatility

Figure 1a shows a dependence of T_g on C^0 for 2448 organic compounds in the training dataset. The compounds with lower C^0 have higher T_g and the T_g appears

158 to level at around 420 K at $C^0 < \sim 10^{-10}$ μg m^{-3}. The dependence of T_g on the atomic O:C
159 ratio is weaker (Fig. 1a and Fig. S2), in agreement with previous studies (Koop et al.,
160 2011; Shiraiwa et al., 2017). Note that a tight correlation between T_g and the O:C ratio
161 has been observed for oxidation products formed from specific precursors including α-
162 pinene (Dette et al., 2014), *n*-heptadecane and naphthalene (Saukko et al., 2012). Based
163 on the trend shown in Fig. 1a, we develop a parameterization (Eq. 1) to predict T_g as a
164 function of C^0 and O:C, which are the parameters used in the two-dimensional VBS
165 (2D-VBS) framework (Donahue et al., 2011).
166
167 $$T_g = 289.10 - 16.50 \times \log_{10}(C^0) - 0.29 \times [\log_{10}(C^0)]^2 + 3.23 \times \log_{10}(C^0)\ (\mathrm{O{:}C}) \quad (1)$$
168
169 The coefficients in Eq. (1) are obtained by fitting the T_g of 2448 compounds in Fig. 1a
170 with multi-linear least squares analysis with 68% prediction and confidence intervals.
171 The predicted T_g by Eq. (1) is plotted in Fig. 1a with the O:C ratios of 0, 0.5, and 1,
172 showing that the predicted dependence of T_g on C^0 follows the trend well in the training
173 dataset. The O:C ratio mainly affects the predicted T_g of volatile or extremely low
174 volatile compounds. Figure 1b shows that the T_g values of those compounds are
175 predicted well by Eq. (1) as indicated by a high correlation coefficient (R) of 0.92. The
176 average absolute value of the relative error (AAVRE, Aiken et al., 2007) is 12%.
177 Equation (1) is further evaluated using the test dataset for SOA components.
178 Figure 1(c) compares T_g predicted by Eq. (1) with estimated T_g from T_m applying the
179 Boyer-Kauzmann rule, showing that Eq. (1) also presents a good performance for
180 predicting T_g of these SOA components with R = 0.96 and AAVRE = 6 %. Note that
181 C^0 values of SOA components were estimated using the EVAPORATION model
182 (Compernolle et al., 2011). The T_g values of individual SOA compounds can be
183 predicted within ±20 K as indicated by the prediction band (dotted lines in Fig. 1c);
184 however, this uncertainty may be much smaller for multicomponent SOA mixtures
185 under ideal mixing conditions as indicated in the confidence band (dashed lines, almost

overlapping with the 1:1 line) (Shiraiwa and Li et al., 2017; DeRieux and Li et al., 2018; Song et al., 2019).

We also develop a parameterization (Eq. 2) predicting T_g as a function of C^0 solely, which can be applied to the information available with the one-dimensional VBS framework (1D-VBS; Donahue et al., 2006), and can be used when the O:C ratio is not available in measurements.

$$T_g = 288.70 - 15.33 \times \log_{10}(C^0) - 0.33 \times [\log_{10}(C^0)]^2 \quad (2)$$

The coefficients in Eq. (2) are obtained following the procedures developing Eq. (1) and the same training dataset is used. Figures S3-S4 show that Eq. (2) gives very similar predictions as Eq. (1) particularly for the compounds with low O:C ratio. As Eq. (1) and (2) are developed based on the compounds with their C^0 higher than ~10^{-20} μg m^{-3}, Eqs. (1–2) may not be applicable for compounds with C^0 < ~10^{-20} μg m^{-3} (Fig. 1a).

2.3 Predictions of T_g and viscosity of organic aerosols

For the application of T_g parameterizations in field observations of volatility distributions, T_g for each volatility bin ($T_{g,i}$) is calculated by Eq. (1). The term volatility refers to the effective saturation mass concentration (C^*) and we assume ideal thermodynamic mixing in which case C^* is equal to C^0 (Donahue et al., 2011). Note that there may be additional uncertainty in application of T_g parameterizations (which were developed based on pure compounds) to each volatility bin representing surrogate of complex multicomponent mixtures. The isolines in Fig. 2 show the $T_{g,i}$ predicted by Eq. (1) with the C^* and O:C defined in the 2D-VBS framework. T_g would be below ~ 250 K for intermediate volatility organic compounds (IVOC; 300 < C^0 < 3×10^6 μg m^{-3}), from ~ 260 K to 290 K for semi-volatile organic compounds (SVOC; 0.3 < C^0 < 300 μg m^{-3}), and higher than 300 K for low-volatile organic compounds (LVOC; 3×10^{-4} < C^0 < 0.3 μg m^{-3}) and extremely low-volatile organic compounds (ELVOC; C^0 < 3×10^{-}

^{4} μg m^{-3}). The T_g increases as the O:C ratio increases for SVOC and IVOC, which is consistent with previous studies (Koop et al., 2011; Saukko et al., 2012; Berkemeier et al., 2014). The T_g slightly decreases as the O:C ratio increases for LVOC and ELVOC compounds, which might be due to the uncertainties in Eq. (1) which is derived from a dataset containing fewer LVOC and ELVOC compounds as shown in Fig. 1a, which exhibits lower T_g with higher O:C.

The glass transition temperatures of organic aerosols under dry conditions ($T_{g,org}$) are calculated by the Gordon-Taylor equation (Gordon and Taylor, 1952) assuming the Gordon-Taylor constant (k_{GT}) of 1 (Dette et al., 2014):

$$T_{g,org} = \sum_i w_i T_{g,i} \quad (3)$$

where w_i is the mass fraction in the particle phase for each volatility bin. The Gordon-Taylor approach has been validated for a wide range of mixtures including SOA compounds (Dette et al., 2014; Lessmeier et al., 2018). The Gordon-Taylor approach may fail in the case of adduct or complex formation (Koop et al., 2011), which is highly unlikely in multicomponent mixtures with myriads of SOA compounds with very small individual mole fractions and thus particular interactions between individual compounds are more likely to average out (Shiraiwa et al., 2017); this aspect would need to be investigated in future studies.

The phase state of aerosol particles strongly depends on their water content (Mikhailov et al., 2009; Koop et al., 2011). Under humid conditions, the water content in OA can be estimated using the effective hygroscopicity parameter (κ) (Petters and Kreidenweis, 2007). The T_g of organic-water mixtures ($T_g(w_{org})$) at given RH can be estimated using the Gordon-Taylor equation (Gordon and Taylor, 1952):

$$T_g(w_{org}) = \frac{(1-w_{org})T_{g,w} + \frac{1}{k_{GT}} w_{org} T_{g,org}}{(1-w_{org}) + \frac{1}{k_{GT}} w_{org}} \quad (4)$$

where w_{org} is the mass fraction of organics in particles; $T_{g,w}$ is the glass transition temperature of pure water (136 K, Kohl et al., 2005), and k_{GT} is the Gordon-Taylor constant for organic-water mixtures which is suggested to be 2.5 (Zobrist et al., 2008; Koop et al., 2011). Viscosity can then be calculated applying the Vogel-Tammann-Fulcher (VTF) equation (Angell, 1991): $\eta = \eta_\infty e^{\frac{T_0 D}{T-T_0}}$, where η_∞ is the viscosity at infinite temperature (10^{-5} Pa s, Angell, 1991), D is the fragility parameter which is assumed to be 10 (DeRieux and Li et al., 2018), and T_0 is the Vogel temperature calculated as $T_0 = \frac{39.17\, T_g}{D+39.17}$.

3. Application in field observations

3.1 Southern Oxidant and Aerosol Study (SOAS)

In this section we predict glass transition temperatures and phase state of ambient OA during the SOAS campaign which took place in the southeastern United States (Centreville, Alabama) in summer 2013 (Carlton et al., 2018). The T_g of organic aerosols under dry conditions ($T_{g,org}$) is calculated using Eqs. (1) and (3) with measured volatility distributions. Figure 2 shows the calculated $T_{g,org}$ placed in the 2D-VBS framework against the average $\log_{10}(C^*)$ calculated by $\sum_i w_i \, log_{10}(C_i^*)$ (Kostenidou et al., 2018) and the measured O:C ratio is from Xu et al. (2015).

Figure 2 shows that $T_{g,org}$ of total OA (TOA) range from 232 K to 334 K, depending on volatility distributions measured by different methods, while the most credible predicted $T_{g,org}$ values span in the range of 313 – 330 K. The reasons are stated below by comparing the different methods deriving the C^* distributions. Stark et al. (2017) used three methods ("Thermograms", "Partitioning" and "Formulas") to derive volatility distributions applying the measurements of organic acids (which were shown to account for about half of the total OA; Yatavelli et al., 2015) from a high-resolution chemical ionization time-of-flight mass spectrometer equipped with a filter inlet for gases and aerosols (Lopez-Hilfiker et al., 2014; Thomson et al., 2017). In the

"Thermogram" method, C^* at 298 K is estimated from the desorption temperature after calibration with known species (Faulhaber et al., 2009). This method results in 93% of OA mass distributed in the LVOC and ELVOC (Stark et al., 2017), and a high $T_{g,org}$ of 330 K is predicted (Fig. 2). While this method may be influenced by thermal decomposition, the peak temperatures of decomposing species can be expected to relate closer to actual volatilities than any of the other two analysis methods (Stark et al., 2017). The result from the thermogram method is consistent with those measured by an aerosol mass spectrometer (AMS) with a thermo denuder, which also applied the thermogram method to estimate the C^* distributions (Hu et al., 2016). Saha et al. (2017) applied an evaporation kinetic model (Lee et al., 2011) based on the VBS approach to extract the C^* distributions, and the effects of enthalpy of vaporization and accommodation coefficient (α) are considered, resulting in the estimated $T_{g,org}$ of 313 K. This study retrieved α of ~0.5, which is consistent with recent experiments (Krechmer et al., 2017; Liu et al., 2019).

The lower $T_{g,org}$ values (< 280 K) calculated from the C^* distributions estimated from the "Formulas" and "Partitioning" methods (Stark et al., 2017) are less atmospherically relevant. The "Formulas" method used the SIMPOL group contribution method (Pankow and Asher, 2008) to calculate vapor pressures from the composition of the identified ions. While the specific functional group distributions needed for SIMPOL are unknown from mass spectrometer measurements, some assumptions can be made, leading to limits in the volatility distributions, all of which showing the same behavior of high volatilities (Stark et al., 2017). This is because many of the detected species can be thermal decomposition products rather than actual SOA molecules (Stark et al., 2015; Stark et al., 2017), which can lead to overestimations of volatilities, resulting in the unlikely low $T_{g,org}$ of 232 K. The "Partitioning" method used the measured particle-phase mass fractions of each species to estimate C^* based on the partitioning theory (Pankow, 1994). The estimated C^* is distributed mainly in the SVOC range (Stark et al., 2017), leading to a $T_{g,org}$ of 279 K (Fig. 2). This value is very

close to the $T_{g,org}$ (281 K) simulated by a global chemical transport model EMAC-ORACLE in which a narrow distribution of C^* (1, 10, 10^2, and 10^3 μg m^{-3}) was applied (Shiraiwa et al., 2017). However, Stark et al. (2017) note that the partitioning-based volatility distribution is likely too high due to an artifact of signal-to-noise limitations, confining the C^* characterizable by the partitioning method to a relatively narrow range centered around the ambient OA concentration (by definition, the semi-volatile range). These analyses indicate that the volatility distributions derived from different methods, even when based on the same measurements, significantly affect the predicted $T_{g,org}$, and the most atmospherically relevant volatility distributions should be carefully chosen to reasonably predict the glass transition temperature of ambient OA. In summary, the $T_{g,org}$ values during the SOAS campaign should be in the range of 313 – 330 K.

Figure 2 also includes $T_{g,org}$ of isoprene-epoxydiols-derived SOA (IEPOX-SOA) identified via positive matrix factorization (PMF) of AMS mass spectra (Lanz et al., 2007). IEPOX-SOA is predicted to have a $T_{g,org}$ of 345 K with very low volatility with the average C^* lower than 10^{-4} μg m^{-3} (Hu et al., 2016; Lopez-Hilfiker et al., 2016; D'Ambro et al., 2019), which may be due to substantial formation of organosulfates and other oligomers (Lin et al., 2012; Hu et al., 2015; Riva et al., 2019). The predicted $T_{g,org}$ of IEPOX-SOA is higher than previously reported $T_{g,org}$ of 263 - 293 K for monoterpene-derived (α-pinene, Δ^3-carene, myrcene, limonene and ocimene) SOA (Petters et al., 2019).

We further calculate the viscosity of OA based on the $T_{g,org}$ of TOA predicted above in order to compare with the ambient phase state measurements during the SOAS campaign. Figure 3(a) shows the predicted viscosity of total OA at different RH. T is adopted as 298 K, the average value during the SOAS campaign (Hu et al., 2016). The effective hygroscopicity parameter (κ) is set to 0.14 for TOA based on measurements (Cerully et al., 2015). The characteristic timescale of mass transport and mixing by molecular diffusion (τ_{mix}) is also calculated: $\tau_{mix} = d_p^2 / (4\pi^2 D_b)$ (Seinfeld and Pandis,

2006), where d_p is the particle diameter and the bulk diffusion coefficient D_b is calculated from the predicted viscosity by the fractional Stokes–Einstein relation (Evoy et al., 2019). We assume the radius of the diffusing molecule of 10^{-10} m and the particle diameter of 200 nm (Shiraiwa et al., 2011). Note that these estimated timescales represent rough estimations, as molecular interactions in complex mixtures are not considered.

The viscosity of TOA at RH of 83% (average RH during SOAS) is predicted to be less than 10^2 Pa s with τ_{mix} less than 1 s, which is consistent with the particle bounce measurements suggesting that organic-dominated particles were mostly liquid during the SOAS campaign (Pajunoja et al., 2016). When RH was below ~50% in the sampling inlet, the particles were found to adopt a semi-solid state (Pajunoja et al., 2016), which agrees with the predicted viscosity of $10^7 – 10^{11}$ Pa s and τ_{mix} can be higher than 1 hour at 50% RH (Fig. 3a). The variations in $T_{g,org}$ (313 – 330 K) due to the different measured C^* distributions (Fig. 2) have a more significant impact on the predicted viscosity at low and medium RH (Fig. 3a). When RH is higher than ~70 %, the predicted viscosities calculated from different $T_{g,org}$ values are very close; at high RH the condensed phase water has a larger influence on the phase state than the volatility does, depending on the hygroscopicity of organic aerosols.

Figure 3 (b) shows diurnal variations of predicted viscosity of total OA using measured T and RH during the SOAS campaign (Hu et al., 2016). During 10:00 – 20:00 when RH < 70 % and T > 298 K, three simulations using different $T_{g,org}$ values predict that total OA occur as semi-solid with the predicted viscosity of $10^2 – 10^7$ Pa s and the mixing times less than 1 hour. Particles are predicted to have low viscosity of < 1 Pa s adopting a liquid phase during nighttime. The lowest viscosity occurs around 5:00 – 6:00 with RH > 95 %. Here we did not consider the effects of the diurnal variations of volatility distributions, as they did not vary dramatically over the campaign period (Saha et al., 2017). Besides T and RH, diurnal variation of ambient aerosol phase state also depends on particle chemical composition and mixing states. Organic particles in

Amazon were found to be more viscous at night than the daytime due to the influence of biomass burning that may form non-liquid particles (Bateman et al., 2017). Particles in a mixed forest in northern Michigan were also found more viscous at night despite higher RH than the daytime, due to the formation of high molar mass organic compounds and smaller inorganic sulfate mass fractions (Slade et al., 2019). Phase state measurements during daytime and nighttime at Atlanta suggested that the ambient particle phase state was influenced by OA composition, the presence of inorganic ions, aerosol liquid water and particle mixing state (Ditto et al., 2019).

3.2 $T_{g,org}$ at 11 global sites

Figure 4 summarizes $T_{g,org}$ at 11 sites where the measured volatility distributions with volatility bins of four or more are available (Table S3). We did not include the data with narrower volatility ranges which may not correctly characterize the properties of ambient SOA (Bilde et al., 2015), and thus may not be appropriate for estimating volatility distributions and it would result in unrealistically low T_g without considering realistically low C^* bins. Note that a narrow VBS may still be useful for efficiency in 3-dimentional chemical transport models for SOA evaporation and condensation under a narrow range of ambient temperature variations (Kostenidou et al., 2018).

Figure 4(a) shows the 2D-VBS framework of O:C vs. $\log_{10}C^*$ with the marker fill color representing $T_{g,org}$, whereas the panel (b) shows $T_{g,org}$ vs. $\log_{10}C^*$ with the marker fill color representing O:C. The marker edge color represents OA components identified via positive matrix factorization of AMS mass spectra (Lanz et al., 2007), including biomass burning OA (BBOA), hydrocarbon-like OA (HOA), cooking OA (COA) and oxygenated OA (OOA) which is sometimes further separated into more oxygenated (MO-OOA) and less oxygenated OA (LO-OOA) factors. Note that these different OA factors may often be internally mixed in ambient atmosphere and predicted $T_{g,org}$ and particle viscosity would be irrelevant in such a case. Nevertheless,

these predictions can be useful when particles are externally mixed or ambient OA are dominated by a certain OA factor.

$T_{g,org}$ of total OA (TOA) varies from 290 K to 339 K. The lower $T_{g,org}$ occurs at Beijing, China in June 2018 (Xu et al., 2019). OA in Beijing was found to be overall more volatile with the particle-phase semi-volatile fraction of 63%. This may be due to the higher total OA mass concentrations in Beijing (Xu et al., 2019), which facilitates greater partitioning of SVOC compounds into the particle phase, leading to a lower $T_{g,org}$. The predicted $T_{g,org}$ of total OA at numerous other sites range between 300 K and 320 K, including Paris (Paciga et al., 2016), Mexico city (Cappa and Jimenez, 2010), Centreville (Hu et al., 2016; Saha et al., 2017; Stark et al., 2017), Raleigh (Saha et al., 2017), and Durham (Saha et al., 2018) in southeastern US. The $T_{g,org}$ value (316 K) at 220 m downwind from a highway in Durham is higher than the $T_{g,org}$ (309 K) at 10 m downwind from a highway due to the dilution and mixing of traffic-sourced particles with background air and evaporation of semi-volatile species during downwind transport (Saha et al., 2018). The $T_{g,org}$ values are predicted to be high with >320 K at the sites in Athens (Louvaris et al., 2017), Pasadena (Ortega et al., 2016), Colorado Rocky Mountain (Stark et al., 2017) and Amazon (Hu et al., 2016). The $T_{g,org}$ values for MO-OOA in Mexico city and Paris are predicted to be very high at ~350 K, reflecting their very low volatility.

Figure 5 shows the OA viscosity variation of OA components against RH. The hygroscopic growth is considered based on hygroscopicity (κ), which is estimated as a function of the O:C ratio (Lambe et al., 2011) when κ was not measured (Table S3). The κ values of OA factors with low O:C ratio, i.e., HOA, COA and BBOA, are estimated to be low (< 0.08); they are predicted to undergo glass transition at RH between 25 % and 68 % and adopt a liquid phase only when RH is very high (~80%). The predicted behavior of BBOA is in line with bounce measurements observing that particles are semisolid in a biomass burning plume (Bateman et al., 2017). OA factors

with higher O:C ratios including LO-OOA, MO-OOA, and IEPOX SOA tend to become liquid (viscosity < 10^2 Pa s) at intermediate RH (Fig. 5b).

There have been growing measurements of RH-dependent viscosity of laboratory-generated SOA formed from different precursors, e.g., isoprene (Song et al., 2015), α-pinene (Abramson et al., 2013; Renbaum-Wolff et al., 2013; Kidd et al., 2014; Pajunoja et al., 2014; Bateman et al., 2015; Zhang et al., 2015; Grayson et al., 2016; Petters et al., 2019), toluene (Song et al., 2016a) and diesel fuel (Song et al., 2019). As the OOA factors characterized from ambient AMS observations may represent ambient SOA (Jimenez et al., 2009), the predicted viscosities of OOA are compared with laboratory measurements of SOA viscosities in Fig. 5b. It shows that the majority of experimental values is well bounded by the predicted viscosities of OOA, represented by the pink shaded area. One exception is the measured viscosity of isoprene SOA is lower than the predicted viscosity of IEPOX SOA at low RH (<30 %). One possible reason is that the isoprene SOA in experiments was formed with high oxidant concentrations with a short reaction time in an oxidation flow reactor in the absence of inorganic seed particles (Song et al., 2015). In ambient environments heterogeneous reactions with acidic sulfate particles forming oligomers are suggested to be an important pathway (Surratt et al., 2010; Lin et al., 2013; Hu et al., 2015; Hu et al., 2016). These particle-phase organosulfates may contribute to a higher viscosity, as indicated by the predicted viscosity of IEPOX-derived organosulfate mixtures with their $T_{g,org}$ estimated to be 313 K (Riva et al., 2019). Another reason could be the mass concentrations of isoprene SOA are much higher (100 ~ 1000 μg m^{-3}, Song et al., 2015) compared to ambient OA concentrations (5 μg m^{-3} during SOAS, Stark et al., 2017). Higher mass concentrations can lead to lower viscosity, as more semi-volatile compounds can partition into the particle phase (Grayson et al., 2016; Jain et al., 2018; Champion et al., 2019).

4. Comparison with global simulations

Shiraiwa et al. (2017) simulated the global distribution of annual averages of SOA phase state using the chemical transport model EMAC (Jöckel et al., 2006) coupled with the organic aerosol module ORACLE (Tsimpidi et al., 2014). ORACLE uses the 1D-VBS framework with four C^* bins (1, 10, 10^2, and 10^3 μg m^{-3}). To estimate T_g the values of molar mass and O:C ratio were assigned for each volatility bin based on molecular corridors (Shiraiwa et al., 2014). Note that the molar mass assigned for the volatility bin of 1 μg m^{-3} was assumed to have relatively high molar mass to partially compensate for the fact that ORACLE does not consider lower volatility bins with higher molar mass. As shown in Fig. 6, global distributions of T_g /T presented in Shiraiwa et al. (2017) is converted to viscosity using the VTF equation. Figure 6 also includes the viscosity of total OA at the 11 sites by applying measured volatility distributions and the global model simulated 5 years' average T and RH with κ assumed to be 0.1 (Pringle et al., 2010). Figure 6b shows that the predicted viscosities at the 11 sites generally agree with the global simulations: the amorphous solid or semi-solid phase occurs over relatively dry areas, including the sites in western US, Mexico City, Beijing and coastal sites in Greece; the lower viscosity occurs in southeastern US and Paris.

The global simulations show that the particles are liquid in the Amazon, while they occur as semi-solid in our predictions based on measured volatility distributions (Fig. 6a). The reason of this disagreement may be mainly due to the substantial fraction of low volatility compounds observed in ambient measurements largely missing from global simulations. Hu et al. (2016) observed that 90 % of OA have volatilities lower than 1 μg m^{-3}, which is the lowest C^* bin in the global simulations. The ambient phase state measurements show that for background conditions of the Amazonian tropical forest, particles are mostly liquid, while with the anthropogenic influence including both urban pollution and biomass burning, they occur as semi-solid or glassy (Bateman et al., 2016; Bateman et al., 2017). The volatility distributions were measured in the dry season heavily influenced by biomass burning (Hu et al., 2016),

464 which can lead to the higher predicted viscosity. Similar cases are observed in Athens
465 and the two sites in the western US, that our predictions based on volatility distributions
466 indicate the glassy phase state while the global model predicts the occurrence of a semi-
467 solid phase.
468
469 **5. Conclusions and implications**
470 We have developed parameterizations to estimate the glass transition
471 temperature of organic compounds using saturation mass concentration (C^0) and atomic
472 O:C ratio. They can be applied to ambient observations of volatility distributions to
473 estimate viscosity of ambient organic aerosols. The T_g and viscosity prediction method
474 can be applied in the volatility basis set or the molecular corridor-based approach to
475 improve OA simulations in chemical transport models by consideration of effects of
476 particle viscosity on OA formation and evolution (Shiraiwa et al., 2017; Pye et al., 2017;
477 Schmedding et al., 2019). Most of the current chemical transport models treat particles
478 as homogeneously well-mixed liquid without considering particle-phase diffusion
479 limitations, which can lead to bias in simulations of SOA mass concentrations and
480 evolution of size distributions (Shiraiwa and Seinfeld, 2012; Zaveri et al., 2018). The
481 SOA simulations applying the VBS framework have not yet included the effects of
482 viscosity on SOA formation and evolution. When the gas-particle partitioning is limited
483 by bulk diffusion, kinetic treatments of SOA partitioning may need to be applied
484 (Perraud et al., 2012; Liu et al., 2016; Yli-Juuti et al., 2017; Li and Shiraiwa, 2019).
485 Some chamber experiments probing the mixing timescales of SOA particles formed
486 from isoprene, α-pinene, and limonene did not observe significant kinetic limitations at
487 moderate and high RH under room temperature (Loza et al., 2013; Ye et al., 2016),
488 while kinetic limitations of bulk diffusion of organic molecules in β-caryophyllene
489 SOA have been observed at 75 % RH (Ye et al., 2018), warranting further investigations
490 on the degree of kinetic limitations in ambient tropospheric conditions. In addition, the
491 interplay of diffusion limitations and phase separation impacts heterogeneous and

multiphase chemistry (Vander Wall et al., 2018; DeRieux et al., 2019; Zhou et al., 2019) and gas-particle partitioning (Zuend and Seinfeld, 2012; Shiraiwa et al., 2013; Freedman, 2017; Pye et al., 2017; Gorkowski et al., 2019a). The particle morphology and the degree of non-ideal mixing and liquid-liquid phase separation can evolve upon atmospheric aging (Gorkowski et al., 2019b). These aspects may also need to be considered for better representation of organic aerosols in future studies.

Appendix A: Parameterizations of T_g based on elemental compositions

We recently developed a parameterization (Eq. A1) predicting T_g as a function of the number of carbon (n_C), hydrogen (n_H), and oxygen (n_O) atoms (DeRieux and Li et al., 2018), similar to the formulation used to predict C^0 (Donahue et al., 2011; Li et al., 2016):

$$T_g = (n_C^0 + \ln(n_C))\, b_C + \ln(n_H)\, b_H + \ln(n_C)\ln(n_H)\, b_{CH} + \ln(n_O)\, b_O + \ln(n_C)\ln(n_O)\, b_{CO} \quad (A1)$$

Values of the coefficients [n_C^0, b_C, b_H, b_{CH}, b_O, and b_{CO}] are [1.96, 61.99, -113.33, 28.74, 0, 0] for CH compounds and [12.13, 10.95, -41.82, 21.61, 118.96, -24.38] for CHO compounds. We broaden the parameterizations for CH and CHO compounds (Eq. A1) to the following equations applicable to CHON (Eq. A2) and CHOS compounds (Eq. A3):

$$T_g = (n_C^0 + \ln(n_C))\, b_C + \ln(n_O)\, b_O + \ln(n_N)\, b_N + \ln(n_C)\ln(n_O)\, b_{CO} + \ln(n_C)\ln(n_N)\, b_{CN} + \ln(n_O)\ln(n_N)\, b_{ON} \quad (A2)$$

$$T_g = (n_C^0 + \ln(n_C))\, b_C + \ln(n_O)\, b_O + \ln(n_S)\, b_S + \ln(n_C)\ln(n_O)\, b_{CO} + \ln(n_C)\ln(n_S)\, b_{CS} + \ln(n_O)\ln(n_S)\, b_{OS} \quad (A3)$$

Values of the coefficients [n_C^0, b_C, b_O, b_N, b_{CO}, b_{CN} and b_{ON}] in Eq. (A2) are [5.34, 31.53, -7.06, 134.96, 6.54, -34.36, -15.35] and [n_C^0, b_C, b_O, b_S, b_{CO}, b_{CS} and b_{OS}] in Eq. (A3)

are [1.12, 68.41, 64.95, 35.77, -12.32, -9.85, 13.80], respectively. These values are obtained by fitting the T_g of CHON and CHOS compounds included in the training dataset (Fig. 1a, Table S1) with multi-linear least squares analysis. Figure A1 (a) shows a fair agreement between the predicted T_g using Eq. (A2) and the measured or otherwise estimated T_g with R of 0.55 and relatively large AAVRE of 16 % for CHON compounds in the training dataset. Figure A1 (b) shows a better prediction performance with R of 0.83 and AAVRE of 9 % for 212 CHON compounds included in the test dataset for SOA components with their T_g estimated by the Boyer-Kauzmann rule using the EPI-estimated T_m. Figure A1 (c) shows that Eq. (A3) performs well for the CHOS compounds included in the training dataset with their T_g estimated by the Boyer-Kauzmann rule using the EPI-estimated T_m (R = 0.87, AAVRE = 8 %).

Figure S5 shows the comparison of T_g predicted by the elemental composition (Eqs. A1– A3) with the T_g predicted as a function of C^0 and the O:C ratio (Eq. 1). The agreement between the two sets of parameterizations for nitrogen- and sulfur-containing compounds is not as good as that for CHO compounds, indicating that there are limitations of predicting T_g by the elemental composition for nitrogen- and sulfur-containing compounds with complex elemental compositions and molecular structures. As volatility depends significantly on functional groups contained in a molecule (Pankow and Asher, 2008; Compernolle et al., 2011), predicting T_g by volatility (Eq. 1) indirectly incorporates the molecular structure effects. As there are limited CHON and CHOS compounds with measured T_g available, future experiments measuring more T_g data for nitrogen- and sulfur-containing organics would help improve the T_g parameterizations by elemental composition.

Appendix B: Comparison of T_g predictions with Zhang et al. (2019)

Recently Zhang et al. (2019) developed a semi-empirical parameterization (Eq. B1) using vapor pressure (p_0 in atm) to predict T_g based on measured T_g of 11 SOA compounds:

548

549 $$T_g = 480.1 - \frac{54395}{(log_{10}(p_0) - 1.7929)^2 + 116.49}$$

550 (B1)

551

552 p_0 can be converted to C^0 via $C^0 = (10^6 M\, p_0)/(RT)$, where R is the ideal gas constant (R

553 = 8.2 ×10^{-5} m^3 atm mol^{-1} K^{-1}), M is the molar mass (g mol^{-1}), and T is the temperature

554 (K). Figure B1 compares the measured T_g included in the training dataset shown in Fig.

555 1a to T_g predicted by (a) C^0 and the atomic O:C (Eq. 1), (b) elemental composition (Eqs.

556 A1-A3), and (c) Eq. (B1) by Zhang et al. (2019). While all three methods perform

557 reasonably well, the predictions using elemental composition (Eqs. A1-A3) show better

558 performance (Fig. B1b) with R of 0.93 and AAVRE of 11 %, respectively.

559 The prediction performance is influenced by the training dataset used

560 developing parameterizations of T_g. The compounds shown in Fig. B1 contain mostly

561 carboxylic acid and hydroxyl functional groups (Koop et al., 2011; Rothfuss and

562 Petters, 2017) and are included in the training dataset used developing Eq. (1) and (Eqs.

563 A1-A3). The training dataset used in Zhang et al. (2019) included 11 organic

564 compounds, and their parameterization predicted T_g of isoprene SOA very well (Zhang

565 et al., 2019), while underpredicted some low-T_g compounds (Fig. B1c). For compounds

566 with their measured T_g higher than 200 K, predictions by Zhang et al. (2019) show good

567 performance and are consistent with the predictions given by Eq. (1) as a function of

568 C^0 and the O:C ratio. Predicted T_g of 2-MT-OS using the three methods are 297 K (Eq.

569 1, as a function of C^0 and the O:C ratio), 275 K (Eq. A3, as a function of the elemental

570 composition) and 280 K (Eq. B1, Zhang et al., 2019), comparable with the measured

571 T_g of 276 ± 15 K (Zhang et al., 2019).

572 Note that predictions using elemental composition (Eq. A1) overestimate the T_g

573 of phthalate compounds (the star markers in Fig. B1). For instance, the observed T_g of

574 dioctyl phthalate is 194 K (Zhang et al., 2018), while the prediction is higher than 300

575 K (Fig. B1b). The reason is that ester is not an effective functional group to increase

viscosity compared to carboxylic acid and hydroxyl (Rothfuss and Petters, 2017). Parameterizations using volatility (Eqs. 1 and B1) improve the predicted T_g of phthalate compounds (Fig. B1a, c). Figure B2 shows compared to the predictions using Eq. (B1) provided in Zhang et al. (2019), predictions by C^0 and the atomic O:C (Eq. 1) and elemental composition (Eq. A1) agree better with the T_g estimated from the Boyer-Kauzmann rule. Future experiments measuring more T_g of SOA components would help verify the T_g predictions by different parameterizations.

Author contribution. YL, JLJ and MS designed the research. YL developed the parameterizations. DAD, HS and JLJ provided measured volatility distributions for the SOAS campaign. YL and MS wrote the manuscript. All authors discussed the results and contributed to manuscript editing.

Data availability. The data used in this study is available in the supplement.

Acknowledgements. This work was funded by the National Science Foundation (AGS-1654104) and the Department of Energy (DE-SC0018349). The CU-Boulder group was supported by DOE (BER/ASR) DE-SC0016559 and NSF AGS-1822664. We thank A. Tsimpidi, V. Karydis, S. Pandis and J. Lelieveld for global simulations of SOA concentrations used to calculate T_g/T (as presented in Shiraiwa et al., 2017), which are converted into viscosity (Fig. 6). We also thank Sergey Nizkorodov, Andreas Zuend, Yue Zhang, Jason Surratt and Markus Petters for stimulating discussions.

References:

Abramson, E., Imre, D., Beranek, J., Wilson, J. M. and Zelenyuk, A.: Experimental determination of chemical diffusion within secondary organic aerosol particles, Phys. Chem. Chem. Phys., 15, 2983-2991, https://doi.org/10.1039/c2cp44013j, 2013.

Aiken, A. C., DeCarlo, P. F. and Jimenez, J. L.: Elemental analysis of organic species with electron ionization high-resolution mass spectrometry, Anal. Chem., 79, 8350-8358, https://doi.org/10.1021/ac071150w, 2007.

Angell, C.: Relaxation in liquids, polymers and plastic crystals—strong/fragile patterns and problems, J. Non-Cryst. Solids, 131-133, 13-31, https://doi.org/10.1016/0022-3093(91)90266-9, 1991.

Bateman, A. P., Bertram, A. K. and Martin, S. T.: Hygroscopic influence on the semisolid-to-liquid transition of secondary organic materials, J. Phys. Chem. A, 119, 4386-4395, https://doi.org/10.1021/jp508521c, 2015.

Bateman, A. P., Gong, Z., Liu, P., Sato, B., Cirino, G., Zhang, Y., Artaxo, P., Bertram, A. K., Manzi, A. O., Rizzo, L. V., Souza, R. A. F., Zaveri, R. A. and Martin, S. T.: Sub-micrometre particulate matter is primarily in liquid form over Amazon rainforest, Nat. Geosci., 9, 34-37, https://doi.org/10.1038/ngeo2599, 2016.

Bateman, A. P., Gong, Z., Harder, T. H., de Sá, S. S., Wang, B., Castillo, P., China, S., Liu, Y., O'Brien, R. E., Palm, B. B., Shiu, H. W., Cirino, G. G., Thalman, R., Adachi, K., Alexander, M. L., Artaxo, P., Bertram, A. K., Buseck, P. R., Gilles, M. K., Jimenez, J. L., Laskin, A., Manzi, A. O., Sedlacek, A., Souza, R. A. F., Wang, J., Zaveri, R. and Martin, S. T.: Anthropogenic influences on the physical state of submicron particulate matter over a tropical forest, Atmos. Chem. Phys., 17, 1759-1773, https://doi.org/10.5194/acp-17-1759-2017, 2017.

Berkemeier, T., Shiraiwa, M., Pöschl, U. and Koop, T.: Competition between water uptake and ice nucleation by glassy organic aerosol particles, Atmos. Chem. Phys., 14, 12513-12531, https://doi.org/10.5194/acp-14-12513-2014, 2014.

Bilde, M., Barsanti, K., Booth, M., Cappa, C. D., Donahue, N. M., Emanuelsson, E. U., McFiggans, G., Krieger, U. K., Marcolli, C., Topping, D., Ziemann, P., Barley, M., Clegg, S., Dennis-Smither, B., Hallquist, M., Hallquist, Å. M., Khlystov, A., Kulmala, M., Mogensen, D., Percival, C. J., Pope, F., Reid, J. P., Ribeiro da Silva, M. A. V., Rosenoern, T., Salo, K., Soonsin, V. P., Yli-Juuti, T., Prisle, N. L., Pagels, J., Rarey, J., Zardini, A. A. and Riipinen, I.: Saturation vapor pressures and transition enthalpies of low-volatility organic molecules of atmospheric relevance: from dicarboxylic acids to complex mixtures, Chem. Rev., 115, 4115-4156, https://doi.org/10.1021/cr5005502, 2015.

Bosse, D.: Diffusion, viscosity, and thermodynamics in liquid systems, Ph.D. thesis, https://kluedo.ub.uni-kl.de/frontdoor/deliver/index/docId/1691/file/PhD-Bosse-published.pdf, 2005.

Boyer, R. F.: Relationship of first-to second-order transition temperatures for crystalline high polymers, J. Appl. Phys., 25, 825-829, https://doi.org/10.1063/1.1721752, 1954.

Cao, W., Knudsen, K., Fredenslund, A. and Rasmussen, P.: Group-contribution viscosity predictions of liquid mixtures using UNIFAC-VLE parameters, Ind. Eng. Chem. Res., 32, 2088–2092, https://doi.org/10.1021/ie00021a034, 1993.

Capouet, M. and Müller, J.-F.: A group contribution method for estimating the vapour pressures of α-pinene oxidation products, Atmos. Chem. Phys., 6, 1455-1467, https://doi.org/10.5194/acp-6-1455-2006, 2006.

Cappa, C. D. and Jimenez, J. L.: Quantitative estimates of the volatility of ambient organic aerosol, Atmos. Chem. Phys., 10, 5409-5424, https://doi.org/10.5194/acp-10-5409-2010, 2010.

Carlton, A. G., de Gouw, J., Jimenez, J. L., Ambrose, J. L., Attwood, A. R., Brown, S., Baker, K. R., Brock, C., Cohen, R. C. and Edgerton, S.: Synthesis of the southeast atmosphere studies: Investigating fundamental atmospheric chemistry questions, Bull. Amer. Meteor. Soc., 99, 547-567, https://doi.org/10.1175/BAMS-D-16-0048.1, 2018.

Cerully, K. M., Bougiatioti, A., Hite Jr, J. R., Guo, H., Xu, L., Ng, N. L., Weber, R. and Nenes, A.: On the link between hygroscopicity, volatility, and oxidation state of ambient and water-soluble aerosols in the southeastern United States, Atmos. Chem. Phys., 15, 8679-8694, https://doi.org/10.5194/acp-15-8679-2015, 2015.

Champion, W. M., Rothfuss, N. E., Petters, M. D. and Grieshop, A. P.: Volatility and viscosity are correlated in terpene secondary organic aerosol formed in a flow reactor, Environ. Sci. Technol. Lett., 6, 513-519, https://doi.org/10.1021/acs.estlett.9b00412, 2019.

Chenyakin, Y., Ullmann, D. A., Evoy, E., Renbaum-Wolff, L., Kamal, S. and Bertram, A. K.: Diffusion coefficients of organic molecules in sucrose–water solutions and comparison with Stokes–Einstein predictions, Atmos. Chem. Phys., 17, 2423-2435, https://doi.org/10.5194/acp-17-2423-2017, 2017.

Compernolle, S., Ceulemans, K. and Müller, J. F.: EVAPORATION: a new vapour pressure estimation methodfor organic molecules including non-additivity and intramolecular interactions, Atmos. Chem. Phys., 11, 9431-9450, https://doi.org/10.5194/acp-11-9431-2011, 2011.

D'Ambro, E. L., Schobesberger, S., Gaston, C. J., Lopez-Hilfiker, F. D., Lee, B. H., Liu, J., Zelenyuk, A., Bell, D., Cappa, C. D., Helgestad, T., Li, Z., Guenther, A., Wang, J., Wise, M., Caylor, R., Surratt, J. D., Riedel, T., Hyttinen, N., Salo, V. T., Hasan, G., Kurtén, T., Shilling, J. E. and Thornton, J. A.: Chamber-based insights into the factors controlling epoxydiol (IEPOX) secondary organic aerosol (SOA) yield, composition, and volatility, Atmos. Chem. Phys., 19, 11253-11265, https://doi.org/10.5194/acp-19-11253-2019, 2019.

DeRieux, W.-S. W., Lakey, P. S. J., Chu, Y., Chan, C. K. K., Glicker, H., Smith, J. N., Zuend, A. and Shiraiwa, M.: Effects of phase state and phase separation on dimethylamine uptake of ammonium sulfate and ammonium sulfate–sucrose mixed particles, ACS Earth Space Chem., 3, 1268-1278, https://doi.org/10.1021/acsearthspacechem.9b00142, 2019.

DeRieux, W. S. W., Li, Y., Lin, P., Laskin, J., Laskin, A., Bertram, A. K., Nizkorodov, S. A. and Shiraiwa, M.: Predicting the glass transition temperature and viscosity

of secondary organic material using molecular composition, Atmos. Chem. Phys., 18, 6331-6351, https://doi.org/10.5194/acp-18-6331-2018, 2018.

Dette, H. P., Qi, M., Schröder, D. C., Godt, A. and Koop, T.: Glass-forming properties of 3-methylbutane-1,2,3-tricarboxylic acid and its mixtures with water and pinonic acid, J. Phys. Chem. A, 118, 7024-7033, https://doi.org/10.1021/jp505910w, 2014.

Dette, H. P. and Koop, T.: Glass formation processes in mixed inorganic/organic aerosol particles, J. Phys. Chem. A, 119, 4552-4561, https://doi.org/10.1021/jp5106967, 2015.

Ditto, J. C., Barnes, E. B., Khare, P., Takeuchi, M., Joo, T., Bui, A. A. T., Lee-Taylor, J., Eris, G., Chen, Y., Aumont, B., Jimenez, J. L., Ng, N. L., Griffin, R. J. and Gentner, D. R.: An omnipresent diversity and variability in the chemical composition of atmospheric functionalized organic aerosol, Commun. Chem., 1, https://doi.org/10.1038/s42004-018-0074-3, 2018.

Ditto, J. C., Joo, T., Khare, P., Sheu, R., Takeuchi, M., Chen, Y., Xu, W., Bui, A. A. T., Sun, Y., Ng, N. L. S. and Gentner, D. R.: Effects of molecular-level compositional variability in organic aerosol on phase state and thermodynamic mixing behavior, Environ. Sci. Technol., 53, 13009-13018, https://doi.org/10.1021/acs.est.9b02664, 2019.

Donahue, N., Robinson, A., Stanier, C. and Pandis, S.: Coupled partitioning, dilution, and chemical aging of semivolatile organics, Environ. Sci. Technol., 40, 2635-2643, https://doi.org/10.1021/es052297c, 2006.

Donahue, N., Epstein, S., Pandis, S. and Robinson, A.: A two-dimensional volatility basis set: 1. organic-aerosol mixing thermodynamics, Atmos. Chem. Phys., 11, 3303-3318, https://doi.org/10.5194/acp-11-3303-2011, 2011.

Evoy, E., Maclean, A. M., Rovelli, G., Li, Y., Tsimpidi, A. P., Karydis, V. A., Kamal, S., Lelieveld, J., Shiraiwa, M., Reid, J. P. and Bertram, A. K.: Predictions of diffusion rates of large organic molecules in secondary organic aerosols using the Stokes–Einstein and fractional Stokes–Einstein relations, Atmos. Chem. Phys., 19, 10073-10085, https://doi.org/10.5194/acp-19-10073-2019, 2019.

Faulhaber, A. E., Thomas, B. M., Jimenez, J. L., Jayne, J. T., Worsnop, D. R. and Ziemann, P. J.: Characterization of a thermodenuder-particle beam mass spectrometer system for the study of organic aerosol volatility and composition, Atmos. Meas. Tech., 2, 15-31, https://doi.org/10.5194/amt-2-15-2009, 2009.

Freedman, M. A.: Phase separation in organic aerosol, Chem. Soc. Rev., 46, 7694-7705, https://doi.org/10.1039/c6cs00783j, 2017.

Gervasi, N. R., Topping, D. O. and Zuend, A.: A predictive group-contribution model for the viscosity of aqueous organic aerosol, Atmos. Chem. Phys., 20, 2987-3008, https://doi.org/10.5194/acp-20-2987-2020, 2020.

Goldstein, A. H. and Galbally, I. E.: Known and unexplored organic constituents in the Earth's atmosphere, Environ. Sci. Technol., 41, 1514-1521, https://doi.org/10.1021/es072476p, 2007.

Gordon, M. and Taylor, J. S.: Ideal copolymers and the second-order transitions of synthetic rubbers. i. non-crystalline copolymers, J. Appl. Chem., 2, 493-500, https://doi.org/10.1002/jctb.5010020901, 1952.

Gorkowski, K., Preston, T. C. and Zuend, A.: RH-dependent organic aerosol thermodynamics via an efficient reduced-complexity model, Atmos. Chem. Phys., 19, 13383–13407, https://doi.org/10.5194/acp-2019-495, 2019a.

Gorkowski, K., Donahue, N. M., and Sullivan, R. C.: Aerosol optical tweezers constrain the morphology evolution of liquid-liquid phase-separated atmospheric particles, Chem, 6, 1-17, https://doi.org/10.1016/j.chempr.2019.1010.1018, 2019b.

Grayson, J. W., Zhang, Y., Mutzel, A., Renbaum-Wolff, L., Böge, O., Kamal, S., Herrmann, H., Martin, S. T. and Bertram, A. K.: Effect of varying experimental conditions on the viscosity of α-pinene derived secondary organic material, Atmos. Chem. Phys., 16, 6027-6040, https://doi.org/10.5194/acp-16-6027-2016, 2016.

Hallquist, M., Wenger, J., Baltensperger, U., Rudich, Y., Simpson, D., Claeys, M., Dommen, J., Donahue, N., George, C. and Goldstein, A.: The formation, properties and impact of secondary organic aerosol: current and emerging issues, Atmos. Chem. Phys., 9, 5155–5236, https://doi.org/10.5194/acp-9-5155-2009, 2009.

Hu, W. W., Campuzano-Jost, P., Palm, B. B., Day, D. A., Ortega, A. M., Hayes, P. L., Krechmer, J. E., Chen, Q., Kuwata, M., Liu, Y. J., de Sá, S. S., McKinney, K., Martin, S. T., Hu, M., Budisulistiorini, S. H., Riva, M., Surratt, J. D., St. Clair, J. M., Isaacman-Van Wertz, G., Yee, L. D., Goldstein, A. H., Carbone, S., Brito, J., Artaxo, P., de Gouw, J. A., Koss, A., Wisthaler, A., Mikoviny, T., Karl, T., Kaser, L., Jud, W., Hansel, A., Docherty, K. S., Alexander, M. L., Robinson, N. H., Coe, H., Allan, J. D., Canagaratna, M. R., Paulot, F. and Jimenez, J. L.: Characterization of a real-time tracer for isoprene epoxydiols-derived secondary organic aerosol (IEPOX-SOA) from aerosol mass spectrometer measurements, Atmos. Chem. Phys., 15, 11807-11833, https://doi.org/10.5194/acp-15-11807-2015, 2015.

Hu, W., Palm, B. B., Day, D. A., Campuzano-Jost, P., Krechmer, J. E., Peng, Z., de Sá, S. S., Martin, S. T., Alexander, M. L., Baumann, K., Hacker, L., Kiendler-Scharr, A., Koss, A. R., de Gouw, J. A., Goldstein, A. H., Seco, R., Sjostedt, S. J., Park, J. H., Guenther, A. B., Kim, S., Canonaco, F., Prévôt, A. S. H., Brune, W. H. and Jimenez, J. L.: Volatility and lifetime against OH heterogeneous reaction of ambient isoprene-epoxydiols-derived secondary organic aerosol (IEPOX-SOA), Atmos. Chem. Phys., 16, 11563-11580, https://doi.org/10.5194/acp-16-11563-2016, 2016.

Jain, S., Fischer, B. K. and Petrucci, A. G.: The Influence of absolute mass loading of secondary organic aerosols on their phase state, Atmosphere, 9, 131,

https://doi.org/10.3390/atmos9040131, https://doi.org/10.3390/atmos9040131, 2018.

Jimenez, J. L., Canagaratna, M. R., Donahue, N. M., Prevot, A. S. H., Zhang, Q., Kroll, J. H., DeCarlo, P. F., Allan, J. D., Coe, H., Ng, N. L., Aiken, A. C., Docherty, K. S., Ulbrich, I. M., Grieshop, A. P., Robinson, A. L., Duplissy, J., Smith, J. D., Wilson, K. R., Lanz, V. A., Hueglin, C., Sun, Y. L., Tian, J., Laaksonen, A., Raatikainen, T., Rautiainen, J., Vaattovaara, P., Ehn, M., Kulmala, M., Tomlinson, J. M., Collins, D. R., Cubison, M. J., Dunlea, E. J., Huffman, J. A., Onasch, T. B., Alfarra, M. R., Williams, P. I., Bower, K., Kondo, Y., Schneider, J., Drewnick, F., Borrmann, S., Weimer, S., Demerjian, K., Salcedo, D., Cottrell, L., Griffin, R., Takami, A., Miyoshi, T., Hatakeyama, S., Shimono, A., Sun, J. Y., Zhang, Y. M., Dzepina, K., Kimmel, J. R., Sueper, D., Jayne, J. T., Herndon, S. C., Trimborn, A. M., Williams, L. R., Wood, E. C., Middlebrook, A. M., Kolb, C. E., Baltensperger, U. and Worsnop, D. R.: Evolution of organic aerosols in the atmosphere, Science, 326, 1525-1529, https://doi.org/10.1126/science.1180353, 2009.

Jöckel, P., Tost, H., Pozzer, A., Brühl, C., Buchholz, J., Ganzeveld, L., Hoor, P., Kerkweg, A., Lawrence, M., nbsp, G, Sander, R., Steil, B., Stiller, G., Tanarhte, M., Taraborrelli, D., van Aardenne, J. and Lelieveld, J.: The atmospheric chemistry general circulation model ECHAM5/MESSy1: consistent simulation of ozone from the surface to the mesosphere, Atmos. Chem. Phys., 6, 5067-5104, https://doi.org/10.5194/acp-6-5067-2006, 2006.

Kanakidou, M., Seinfeld, J., Pandis, S., Barnes, I., Dentener, F., Facchini, M., Dingenen, R. V., Ervens, B., Nenes, A. and Nielsen, C.: Organic aerosol and global climate modelling: a review, Atmos. Chem. Phys., 5, 1053-1123, https://doi.org/10.5194/acp-5-1053-2005, 2005.

Kauzmann, W.: The nature of the glassy state and the behavior of liquids at low temperatures, Chem. Rev., 43, 219-256, https://doi.org/10.1021/cr60135a002, 1948.

Kidd, C., Perraud, V., Wingen, L. M. and Finlayson-Pitts, B. J.: Integrating phase and composition of secondary organic aerosol from the ozonolysis of alpha-pinene, Proc. Natl. Acad. Sci. U.S.A., 111, 7552-7557, https://doi.org/10.1073/pnas.1322558111, 2014.

Knopf, D. A., Alpert, P. A. and Wang, B.: The role of organic aerosol in atmospheric ice nucleation: a review, ACS Earth Space Chem., 2, 168-202, https://doi.org/10.1021/acsearthspacechem.7b00120, 2018.

Kohl, I., Bachmann, L., Hallbrucker, A., Mayer, E. and Loerting, T.: Liquid-like relaxation in hyperquenched water at $\leqslant$ 140 K, Phys. Chem. Chem. Phys., 7, 3210-3220, https://doi.org/10.1039/B507651J, 2005.

Koop, T., Bookhold, J., Shiraiwa, M. and Poschl, U.: Glass transition and phase state of organic compounds: dependency on molecular properties and implications

for secondary organic aerosols in the atmosphere, Phys. Chem. Chem. Phys., 13, 19238-19255, https://doi.org/10.1039/C1CP22617G, 2011.

Kostenidou, E., Karnezi, E., Hite Jr, J. R., Bougiatioti, A., Cerully, K., Xu, L., Ng, N. L., Nenes, A. and Pandis, S. N.: Organic aerosol in the summertime southeastern United States: components and their link to volatility distribution, oxidation state and hygroscopicity, Atmos. Chem. Phys., 18, 5799-5819, https://doi.org/10.5194/acp-18-5799-2018, 2018.

Krechmer, J. E., Day, D. A., Ziemann, P. J. and Jimenez, J. L.: Direct measurements of gas/particle partitioning and mass accommodation coefficients in environmental chambers, Environ. Sci. Technol., 51, 11867-11875, https://doi.org/10.1021/acs.est.7b02144, 2017.

Krieger, U. K., Marcolli, C. and Reid, J. P.: Exploring the complexity of aerosol particle properties and processes using single particle techniques, Chem. Soc. Rev., 41, 6631-6662, https://doi.org/10.1039/C2CS35082C, 2012.

Lambe, A. T., Onasch, T. B., Massoli, P., Croasdale, D. R., Wright, J. P., Ahern, A. T., Williams, L. R., Worsnop, D. R., Brune, W. H. and Davidovits, P.: Laboratory studies of the chemical composition and cloud condensation nuclei (CCN) activity of secondary organic aerosol (SOA) and oxidized primary organic aerosol (OPOA), Atmos. Chem. Phys., 11, 8913-8928, https://doi.org/10.5194/acp-11-8913-2011, 2011.

Lanz, V. A., Alfarra, M. R., Baltensperger, U., Buchmann, B., Hueglin, C. and Prévôt, A. S. H.: Source apportionment of submicron organic aerosols at an urban site by factor analytical modelling of aerosol mass spectra, Atmos. Chem. Phys., 7, 1503-1522, https://doi.org/10.5194/acp-7-1503-2007, 2007.

Lee, B.-H., Pierce, J. R., Engelhart, G. J. and Pandis, S. N.: Volatility of secondary organic aerosol from the ozonolysis of monoterpenes, Atmos. Environ., 45, 2443-2452, https://doi.org/10.1016/j.atmosenv.2011.02.004, 2011.

Lessmeier, J., Dette, H. P., Godt, A. and Koop, T.: Physical state of 2-methylbutane-1,2,3,4-tetraol in pure and internally mixed aerosols, Atmos. Chem. Phys., 18, 15841-15857, https://doi.org/10.5194/acp-18-15841-2018, 2018.

Li, Y., Pöschl, U. and Shiraiwa, M.: Molecular corridors and parameterizations of volatility in the chemical evolution of organic aerosols, Atmos. Chem. Phys., 16, 3327-3344, https://doi.org/10.5194/acp-16-3327-2016, 2016.

Li, Y. and Shiraiwa, M.: Timescales of secondary organic aerosols to reach equilibrium at various temperatures and relative humidities, Atmos. Chem. Phys., 19, 5959-5971, https://doi.org/10.5194/acp-19-5959-2019, 2019.

Lin, Y.-H., Zhang, Z., Docherty, K. S., Zhang, H., Budisulistiorini, S. H., Rubitschun, C. L., Shaw, S. L., Knipping, E. M., Edgerton, E. S., Kleindienst, T. E., Gold, A. and Surratt, J. D.: Isoprene epoxydiols as precursors to secondary organic aerosol formation: acid-catalyzed reactive uptake studies with authentic compounds, Environ. Sci. Technol., 46, 250-258, https://doi.org/10.1021/es202554c, 2012.

Lin, Y.-H., Zhang, H., Pye, H. O. T., Zhang, Z., Marth, W. J., Park, S., Arashiro, M., Cui, T., Budisulistiorini, S. H., Sexton, K. G., Vizuete, W., Xie, Y., Luecken, D. J., Piletic, I. R., Edney, E. O., Bartolotti, L. J., Gold, A. and Surratt, J. D.: Epoxide as a precursor to secondary organic aerosol formation from isoprene photooxidation in the presence of nitrogen oxides, Proc. Natl. Acad. Sci. U.S.A., 110, 6718-6723, https://doi.org/10.1073/pnas.1221150110, 2013.

Liu, P., Li, Y. J., Wang, Y., Gilles, M. K., Zaveri, R. A., Bertram, A. K. and Martin, S. T.: Lability of secondary organic particulate matter, Proc. Natl. Acad. Sci. U.S.A., 113, 12643-12648, https://doi.org/10.1021/10.1021/acscentsci.7b00452, 2016.

Liu, X., Day, D. A., Krechmer, J. E., Brown, W., Peng, Z., Ziemann, P. J. and Jimenez, J. L.: Direct measurements of semi-volatile organic compound dynamics show near-unity mass accommodation coefficients for diverse aerosols, Commun. Chem., 2, https://doi.org/10.1038/s42004-019-0200-x, 2019.

Liu, Y., Wu, Z., Wang, Y., Xiao, Y., Gu, F., Zheng, J., Tan, T., Shang, D., Wu, Y., Zeng, L., Hu, M., Bateman, A. P. and Martin, S. T.: Submicrometer particles are in the liquid state during heavy haze episodes in the urban atmosphere of Beijing, China, Environ. Sci. Technol. Lett., 4, 427-432, https://doi.org/10.1021/acs.estlett.7b00352, 2017.

Lopez-Hilfiker, F. D., Mohr, C., Ehn, M., Rubach, F., Kleist, E., Wildt, J., Mentel, T. F., Lutz, A., Hallquist, M., Worsnop, D. and Thornton, J. A.: A novel method for online analysis of gas and particle composition: description and evaluation of a Filter Inlet for Gases and AEROsols (FIGAERO), Atmos. Meas. Tech., 7, 983-1001, https://doi.org/10.5194/amt-7-983-2014, 2014.

Lopez-Hilfiker, F. D., Mohr, C., D'Ambro, E. L., Lutz, A., Riedel, T. P., Gaston, C. J., Iyer, S., Zhang, Z., Gold, A., Surratt, J. D., Lee, B. H., Kurten, T., Hu, W. W., Jimenez, J., Hallquist, M. and Thornton, J. A.: Molecular composition and volatility of organic aerosol in the southeastern U.S.: implications for IEPOX derived SOA, Environ. Sci. Technol., 50, 2200-2209, https://doi.org/10.1021/acs.est.5b04769, 2016.

Louvaris, E. E., Florou, K., Karnezi, E., Papanastasiou, D. K., Gkatzelis, G. I. and Pandis, S. N.: Volatility of source apportioned wintertime organic aerosol in the city of Athens, Atmos. Environ., 158, 138-147, https://doi.org/10.1016/j.atmosenv.2017.03.042, 2017.

Loza, C. L., Coggon, M. M., Nguyen, T. B., Zuend, A., Flagan, R. C. and Seinfeld, J. H.: On the mixing and evaporation of secondary organic aerosol components, Environ. Sci. Technol., 47, 6173-6180, https://doi.org/ 10.1021/es400979k, 2013.

Marshall, F. H., Berkemeier, T., Shiraiwa, M., Nandy, L., Ohm, P. B., Dutcher, C. S. and Reid, J. P.: Influence of particle viscosity on mass transfer and heterogeneous ozonolysis kinetics in aqueous-sucrose-maleic acid aerosol,

Phys. Chem. Chem. Phys., 20, 15560-15573, https://doi.org/10.1039/c8cp01666f, 2018.
Mikhailov, E., Vlasenko, S., Martin, S. T., Koop, T. and Pöschl, U.: Amorphous and crystalline aerosol particles interacting with water vapor: conceptual framework and experimental evidence for restructuring, phase transitions and kinetic limitations, Atmos. Chem. Phys., 9, 9491-9522, https://doi.org/10.5194/acp-9-9491-2009, 2009.
Nizkorodov, S. A., Laskin, J. and Laskin, A.: Molecular chemistry of organic aerosols through the application of high resolution mass spectrometry, Phys. Chem. Chem. Phys., 13, 3612-3629, https://doi.org/10.1039/c0cp02032j, 2011.
O'Brien, R. E., Neu, A., Epstein, S. A., MacMillan, A. C., Wang, B., Kelly, S. T., Nizkorodov, S. A., Laskin, A., Moffet, R. C. and Gilles, M. K.: Physical properties of ambient and laboratory-generated secondary organic aerosol, Geophys. Res. Lett., 41, 4347-4353, https://doi.org/10.1002/2014GL060219, 2014.
O'Meara, S., Booth, A. M., Barley, M. H., Topping, D. and McFiggans, G.: An assessment of vapour pressure estimation methods, Phys.Chem.Chem.Phys., 16, 19453-19469, https://doi.org/10.1039/c4cp00857j, 2014.
Ortega, A. M., Hayes, P. L., Peng, Z., Palm, B. B., Hu, W., Day, D. A., Li, R., Cubison, M. J., Brune, W. H., Graus, M., Warneke, C., Gilman, J. B., Kuster, W. C., de Gouw, J., Gutiérrez-Montes, C. and Jimenez, J. L.: Real-time measurements of secondary organic aerosol formation and aging from ambient air in an oxidation flow reactor in the Los Angeles area, Atmos. Chem. Phys., 16, 7411-7433, 10.5194/acp-16-7411-2016, 2016.
Paciga, A., Karnezi, E., Kostenidou, E., Hildebrandt, L., Psichoudaki, M., Engelhart, G. J., Lee, B. H., Crippa, M., Prévôt, A. S. H., Baltensperger, U. and Pandis, S. N.: Volatility of organic aerosol and its components in the megacity of Paris, Atmos. Chem. Phys., 16, 2013-2023, https://doi.org/10.5194/acp-16-2013-2016, 2016.
Pajunoja, A., Hu, W., Leong, Y. J., Taylor, N. F., Miettinen, P., Palm, B. B., Mikkonen, S., Collins, D. R., Jimenez, J. L. and Virtanen, A.: Phase state of ambient aerosol linked with water uptake and chemical aging in the southeastern US, Atmos. Chem. Phys., 16, 11163-11176, https://doi.org/10.5194/acp-16-11163-2016, 2016.
Pajunoja, A., Malila, J., Hao, L., Joutsensaari, J., Lehtinen, K. E. and Virtanen, A.: Estimating the viscosity range of SOA particles based on their coalescence time, Aerosol Sci. Technol., 48, https://doi.org/10.1080/02786826.2013.870325, 2014.
Pankow, J. F.: An absorption model of gas-particle partitioning of organic-compounds in the atmosphere, Atmos. Environ., 28, 185-188, https://doi.org/10.1016/1352-2310(94)90093-0, 1994.

Pankow, J. F. and Asher, W. E.: SIMPOL.1: a simple group contribution method for predicting vapor pressures and enthalpies of vaporization of multifunctional organic compounds, Atmos. Chem. Phys., 8, 2773-2796, https://doi.org/10.5194/acp-8-2773-2008, 2008.

Perraud, V., Bruns, E. A., Ezell, M. J., Johnson, S. N., Yu, Y., Alexander, M. L., Zelenyuk, A., Imre, D., Chang, W. L., Dabdub, D., Pankow, J. F. and Finlayson-Pitts, B. J.: Nonequilibrium atmospheric secondary organic aerosol formation and growth, Proc. Natl. Acad. Sci. U.S.A., 109, 2836-2841, https://doi.org/10.1073/pnas.1119909109, 2012.

Petters, M. D. and Kreidenweis, S. M.: A single parameter representation of hygroscopic growth and cloud condensation nucleus activity, Atmos. Chem. Phys., 7, 1961-1971, https://doi.org/10.5194/acp-7-1961-2007, 2007.

Petters, S. S., Kreidenweis, S. M., Grieshop, A. P., Ziemann, P. J. and Petters, M. D.: Temperature- and humidity-dependent phase states of secondary organic aerosols, Geophys. Res. Lett., 46, https://doi.org/10.1029/2018GL080563, 2019.

Pöschl, U. and Shiraiwa, M.: Multiphase chemistry at the atmosphere-biosphere interface influencing climate and public health in the anthropocene, Chem. Rev., 115, 4440-4475, https://doi.org/10.1021/cr500487s, 2015.

Price, H. C., Mattsson, J. and Murray, B. J.: Sucrose diffusion in aqueous solution, Phys. Chem. Chem. Phys., 18, 19207-19216, https://doi.org/10.1039/c6cp03238a, 2016.

Pringle, K. J., Tost, H., Pozzer, A., Pöschl, U. and Lelieveld, J.: Global distribution of the effective aerosol hygroscopicity parameter for CCN activation, Atmos. Chem. Phys., 10, 5241-5255, https://doi.org/10.5194/acp-10-5241-2010, 2010.

Pye, H. O. T., Murphy, B. N., Xu, L., Ng, N. L., Carlton, A. G., Guo, H., Weber, R., Vasilakos, P., Appel, K. W., Budisulistiorini, S. H., Surratt, J. D., Nenes, A., Hu, W., Jimenez, J. L., Isaacman-VanWertz, G., Misztal, P. K. and Goldstein, A. H.: On the implications of aerosol liquid water and phase separation for organic aerosol mass, Atmos. Chem. Phys., 17, 343-369, https://doi.org/10.5194/acp-17-343-2017, 2017.

Reid, J. P., Bertram, A. K., Topping, D. O., Laskin, A., Martin, S. T., Petters, M. D., Pope, F. D. and Rovelli, G.: The viscosity of atmospherically relevant organic particles, Nat. Commun., 9, 956, https://doi.org/10.1038/s41467-018-03027-z, 2018.

Renbaum-Wolff, L., Grayson, J. W., Bateman, A. P., Kuwata, M., Sellier, M., Murray, B. J., Shilling, J. E., Martin, S. T. and Bertram, A. K.: Viscosity of α-pinene secondary organic material and implications for particle growth and reactivity, Proc. Natl. Acad. Sci. U.S.A., 110, 8014-8019, https://doi.org/10.1073/pnas.1219548110, 2013.

Riva, M., Chen, Y., Zhang, Y., Lei, Z., Olson, N. E., Boyer, H. C., Narayan, S., Yee, L. D., Green, H. S., Cui, T., Zhang, Z., Baumann, K., Fort, M., Edgerton, E.,

Budisulistiorini, S. H., Rose, C. A., Ribeiro, I. O., e Oliveira, R. L., dos Santos, E. O., Machado, C. M. D., Szopa, S., Zhao, Y., Alves, E. G., de Sá, S. S., Hu, W., Knipping, E. M., Shaw, S. L., Duvoisin Junior, S., de Souza, R. A. F., Palm, B. B., Jimenez, J.-L., Glasius, M., Goldstein, A. H., Pye, H. O. T., Gold, A., Turpin, B. J., Vizuete, W., Martin, S. T., Thornton, J. A., Dutcher, C. S., Ault, A. P. and Surratt, J. D.: Increasing isoprene epoxydiol-to-inorganic sulfate aerosol ratio results in extensive conversion of inorganic sulfate to organosulfur forms: implications for aerosol physicochemical properties, Environ. Sci. Technol., 53, 8682-8694, https://doi.org/10.1021/acs.est.9b01019, 2019.

Rothfuss, N. E. and Petters, M. D.: Influence of functional groups on the viscosity of organic aerosol, Environ. Sci. Technol., 51, 271-279, https://doi.org/10.1021/acs.est.6b04478, 2017.

Rovelli, G., Song, Y.-C., Maclean, A. M., Topping, D. O., Bertram, A. K. and Reid, J. P.: Comparison of approaches for measuring and predicting the viscosity of ternary component aerosol particles, Anal. Chem., 91, 5074-5082, https://doi.org/10.1021/acs.analchem.8b05353, 2019.

Saha, P. K., Khlystov, A., Yahya, K., Zhang, Y., Xu, L., Ng, N. L. and Grieshop, A. P.: Quantifying the volatility of organic aerosol in the southeastern US, Atmos. Chem. Phys., 17, 501-520, https://doi.org/10.5194/acp-17-501-2017, 2017.

Saha, P. K., Khlystov, A. and Grieshop, A. P.: Downwind evolution of the volatility and mixing state of near-road aerosols near a US interstate highway, Atmos. Chem. Phys., 18, 2139-2154, https://doi.org/10.5194/acp-18-2139-2018, 2018.

Saukko, E., Lambe, A. T., Massoli, P., Koop, T., Wright, J. P., Croasdale, D. R., Pedernera, D. A., Onasch, T. B., Laaksonen, A., Davidovits, P., Worsnop, D. R. and Virtanen, A.: Humidity-dependent phase state of SOA particles from biogenic and anthropogenic precursors, Atmos. Chem. Phys., 12, 7517-7529, https://doi.org/10.5194/acp-12-7517-2012, 2012.

Schmedding, R., Rasool, Q. Z., Zhang, Y., Pye, H. O. T., Zhang, H., Chen, Y., Surratt, J. D., Lee, B. H., Mohr, C., Lopez-Hilfiker, F. D., Thornton, J. A., Goldstein, A. H. and Vizuete, W.: Predicting secondary organic aerosol phase state and viscosity and its effect on multiphase chemistry in a regional scale air quality model, Atmos. Chem. Phys. Discuss., 2019, 1-59, https://doi.org/10.5194/acp-2019-900, 2019.

Schum, S. K., Zhang, B., Džepina, K., Fialho, P., Mazzoleni, C. and Mazzoleni, L. R.: Molecular and physical characteristics of aerosol at a remote free troposphere site: implications for atmospheric aging, Atmos. Chem. Phys., 18, 14017-14036, https://doi.org/10.5194/acp-18-14017-2018, 2018.

Seinfeld, J. H. and Pandis, S. N.: Atmospheric chemistry and physics - From air pollution to climate change, John Wiley & Sons, Inc., New York, 2006.

Shiraiwa, M., Ammann, M., Koop, T. and Poschl, U.: Gas uptake and chemical aging of semisolid organic aerosol particles, Proc. Natl. Acad. Sci. U.S.A., 108, 11003-11008, https://doi.org/10.1073/pnas.1103045108, 2011.

Shiraiwa, M. and Seinfeld, J. H.: Equilibration timescale of atmospheric secondary organic aerosol partitioning, Geophys. Res. Lett., 39, https://doi.org/10.1029/2012GL054008, 2012.

Shiraiwa, M., Zuend, A., Bertram, A. K. and Seinfeld, J. H.: Gas-particle partitioning of atmospheric aerosols: interplay of physical state, non-ideal mixing and morphology, Phys. Chem. Chem. Phys., 15, 11441-11453, https://doi.org/10.1039/C3CP51595H, 2013.

Shiraiwa, M., Berkemeier, T., Schilling-Fahnestock, K. A., Seinfeld, J. H. and Pöschl, U.: Molecular corridors and kinetic regimes in the multiphase chemical evolution of secondary organic aerosol, Atmos. Chem. Phys., 14, 8323-8341, https://doi.org/10.5194/acp-14-8323-2014, 2014.

Shiraiwa, M., Li, Y., Tsimpidi, A. P., Karydis, V. A., Berkemeier, T., Pandis, S. N., Lelieveld, J., Koop, T. and Pöschl, U.: Global distribution of particle phase state in atmospheric secondary organic aerosols, Nat. Commun., 8, 15002, https://doi.org/10.1038/ncomms15002, 2017.

Shrivastava, M., Cappa, C. D., Fan, J., Goldstein, A. H., Guenther, A. B., Jimenez, J. L., Kuang, C., Laskin, A., Martin, S. T., Ng, N. L., Petaja, T., Pierce, J. R., Rasch, P. J., Roldin, P., Seinfeld, J. H., Shilling, J., Smith, J. N., Thornton, J. A., Volkamer, R., Wang, J., Worsnop, D. R., Zaveri, R. A., Zelenyuk, A. and Zhang, Q.: Recent advances in understanding secondary organic aerosol: Implications for global climate forcing, Rev. Geophys., 55, 509-559, https://doi.org/10.1002/2016RG000540, 2017.

Slade, J. H., Ault, A. P., Bui, A. T., Ditto, J. C., Lei, Z., Bondy, A. L., Olson, N. E., Cook, R. D., Desrochers, S. J., Harvey, R. M., Erickson, M. H., Wallace, H. W., Alvarez, S. L., Flynn, J. H., Boor, B. E., Petrucci, G. A., Gentner, D. R., Griffin, R. J. and Shepson, P. B.: Bouncier particles at night: biogenic secondary organic aerosol chemistry and sulfate drive diel variations in the aerosol phase in a mixed forest, Environ. Sci. Technol., 53, 4977-4987, https://doi.org/10.1021/acs.est.8b07319, 2019.

Song, M., Liu, P. F., Hanna, S. J., Li, Y. J., Martin, S. T. and Bertram, A. K.: Relative humidity-dependent viscosities of isoprene-derived secondary organic material and atmospheric implications for isoprene-dominant forests, Atmos. Chem. Phys., 15, 5145-5159, https://doi.org/10.5194/acp-15-5145-2015, 2015.

Song, M., Liu, P. F., Hanna, S. J., Zaveri, R. A., Potter, K., You, Y., Martin, S. T. and Bertram, A. K.: Relative humidity-dependent viscosity of secondary organic material from toluene photo-oxidation and possible implications for organic particulate matter over megacities, Atmos. Chem. Phys., 16, 8817-8830, https://doi.org/10.5194/acp-16-8817-2016, 2016a.

Song, M., Maclean, A. M., Huang, Y., Smith, N. R., Blair, S. L., Laskin, J., Laskin, A., DeRieux, W. S. W., Li, Y., Shiraiwa, M., Nizkorodov, S. A. and Bertram, A. K.: Liquid-liquid phase separation and viscosity within secondary organic

aerosol generated from diesel fuel vapors, Atmos. Chem. Phys., 19, 12515–12529, https://doi.org/10.5194/acp-2019-367, 2019.

Song, Y. C., Haddrell, A. E., Bzdek, B. R., Reid, J. P., Bannan, T., Topping, D. O., Percival, C. and Cai, C.: Measurements and predictions of binary component aerosol particle viscosity, J. Phys. Chem. A, 120, 8123-8137, https://doi.org/10.1021/acs.jpca.6b07835, 2016b.

Stark, H., Yatavelli, R. L. N., Thompson, S. L., Kimmel, J. R., Cubison, M. J., Chhabra, P. S., Canagaratna, M. R., Jayne, J. T., Worsnop, D. R. and Jimenez, J. L.: Methods to extract molecular and bulk chemical information from series of complex mass spectra with limited mass resolution, Int. J. Mass Spectrom., 389, 26-38, https://doi.org/10.1016/j.ijms.2015.08.011, 2015.

Stark, H., Yatavelli, R. L., Thompson, S. L., Kang, H., Krechmer, J. E., Kimmel, J. R., Palm, B. B., Hu, W., Hayes, P. L. and Day, D. A.: Impact of thermal decomposition on thermal desorption instruments: advantage of thermogram analysis for quantifying volatility distributions of organic species, Environ. Sci. Technol., 51, 8491-8500, https://doi.org/10.1021/acs.est.7b00160, 2017.

Surratt, J. D., Chan, A. W. H., Eddingsaas, N. C., Chan, M., Loza, C. L., Kwan, A. J., Hersey, S. P., Flagan, R. C., Wennberg, P. O. and Seinfeld, J. H.: Reactive intermediates revealed in secondary organic aerosol formation from isoprene, Proc. Natl. Acad. Sci. U.S.A., 107, 6640-6645, https://doi.org/10.1073/pnas.0911114107, 2010.

Thomas, L. H., Meatyard, R., Smith, H. and Davies, G. H.: Viscosity behavior of associated liquids at lower temperatures and vapor pressures, J. Chem. Eng. Data, 24, 161-164, https://doi.org/10.1021/je60082a011, 1979.

Thompson, S. L., Yatavelli, R. L. N., Stark, H., Kimmel, J. R., Krechmer, J. E., Day, D. A., Hu, W., Isaacman-VanWertz, G., Yee, L., Goldstein, A. H., Khan, M. A. H., Holzinger, R., Kreisberg, N., Lopez-Hilfiker, F. D., Mohr, C., Thornton, J. A., Jayne, J. T., Canagaratna, M., Worsnop, D. R. and Jimenez, J. L.: Field intercomparison of the gas/particle partitioning of oxygenated organics during the Southern Oxidant and Aerosol Study (SOAS) in 2013, Aerosol Sci. Tech., 51, 30-56, https://doi.org/10.1080/02786826.2016.1254719, 2017.

Tsimpidi, A. P., Karydis, V. A., Pozzer, A., Pandis, S. N. and Lelieveld, J.: ORACLE (v1.0): module to simulate the organic aerosol composition and evolution in the atmosphere, Geosci. Model Dev., 7, 3153-3172, https://doi.org/10.5194/gmd-7-3153-2014, 2014.

US EPA: Estimation Programs Interface Suite™ for Microsoft Windows v4.1, United States Environmental Protection Agency, Washington, DC, USA, 2015.

Vander Wall, A. C., Lakey, P. S. J., Rossich Molina, E., Perraud, V., Wingen, L. M., Xu, J., Soulsby, D., Gerber, R. B., Shiraiwa, M. and Finlayson-Pitts, B. J.: Understanding interactions of organic nitrates with the surface and bulk of organic films: implications for particle growth in the atmosphere, Environ. Sci.

Processes Impacts, 20, 1593-1610, https://doi.org/10.1039/C8EM00348C, 2018.

Virtanen, A., Joutsensaari, J., Koop, T., Kannosto, J., YliPirilä, P., Leskinen, J., Mäkelä, J. M., Holopainen, J. K., Pöschl, U., Kulmala, M., Worsnop, D. R. and Laaksonen, A.: An amorphous solid state of biogenic secondary organic aerosol particles, Nature, 467, 824-827, https://doi.org/10.1038/nature09455, 2010.

Xu, L., Suresh, S., Guo, H., Weber, R. J. and Ng, N. L.: Aerosol characterization over the southeastern United States using high-resolution aerosol mass spectrometry: spatial and seasonal variation of aerosol composition and sources with a focus on organic nitrates, Atmos. Chem. Phys., 15, 7307-7336, https://doi.org/10.5194/acp-15-7307-2015, 2015.

Xu, W., Xie, C., Karnezi, E., Zhang, Q., Wang, J., Pandis, S. N., Ge, X., Zhang, J., An, J., Wang, Q., Zhao, J., Du, W., Qiu, Y., Zhou, W., He, Y., Li, Y., Li, J., Fu, P., Wang, Z., Worsnop, D. R. and Sun, Y.: Summertime aerosol volatility measurements in Beijing, China, Atmos. Chem. Phys., 19, https://doi.org/10205-10216, 10.5194/acp-19-10205-2019, 2019.

Yatavelli, R. L. N., Mohr, C., Stark, H., Day, D. A., Thompson, S. L., Lopez-Hilfiker, F. D., Campuzano-Jost, P., Palm, B. B., Vogel, A. L., Hoffmann, T., Heikkinen, L., Äijälä, M., Ng, N. L., Kimmel, J. R., Canagaratna, M. R., Ehn, M., Junninen, H., Cubison, M. J., Petäjä, T., Kulmala, M., Jayne, J. T., Worsnop, D. R. and Jimenez, J. L.: Estimating the contribution of organic acids to northern hemispheric continental organic aerosol, Geophys. Res. Lett., 42, 6084-6090, https://doi.org/10.1002/2015gl064650, 2015.

Ye, Q., Robinson, E. S., Ding, X., Ye, P., Sullivan, R. C. and Donahue, N. M.: Mixing of secondary organic aerosols versus relative humidity, Proc. Natl. Acad. Sci. U.S.A., 113, 12649-12654, https://doi.org/10.1073/pnas.1604536113, 2016.

Ye, Q., Upshur, M. A., Robinson, E. S., Geiger, F. M., Sullivan, R. C., Thomson, R. J. and Donahue, N. M.: Following particle-particle mixing in atmospheric secondary organic aerosols by using isotopically labeled terpenes, Chem, 4, 318-333, https://doi.org/10.1016/j.chempr.2017.12.008, 2018.

Yli-Juuti, T., Pajunoja, A., Tikkanen, O.-P., Buchholz, A., Faiola, C., Väisänen, O., Hao, L., Kari, E., Peräkylä, O., Garmash, O., Shiraiwa, M., Ehn, M., Lehtinen, K. and Virtanen, A.: Factors controlling the evaporation of secondary organic aerosol from α-pinene ozonolysis, Geophys. Res. Lett., 44, 2562-2570, https://doi.org/10.1002/2016GL072364, 2017.

Zaveri, R. A., Shilling, J. E., Zelenyuk, A., Liu, J., Bell, D. M., D'Ambro, E. L., Gaston, C. J., Thornton, J. A., Laskin, A., Lin, P., Wilson, J., Easter, R. C., Wang, J., Bertram, A. K., Martin, S. T., Seinfeld, J. H. and Worsnop, D. R.: Growth kinetics and size distribution dynamics of viscous secondary organic aerosol, Environ. Sci. Technol., 52, 1191-1199, https://doi.org/10.1021/acs.est.7b04623, 2018.

Zhang, Y., Sanchez, M. S., Douet, C., Wang, Y., Bateman, A. P., Gong, Z., Kuwata, M., Renbaum-Wolff, L., Sato, B. B., Liu, P. F., Bertram, A. K., Geiger, F. M. and Martin, S. T.: Changing shapes and implied viscosities of suspended submicron particles, Atmos. Chem. Phys., 15, 7819-7829, https://doi.org/10.5194/acp-15-7819-2015, 2015.

Zhang, Y., Katira, S., Lee, A., Lambe, A. T., Onasch, T. B., Xu, W., Brooks, W. A., Canagaratna, M. R., Freedman, A. and Jayne, J. T.: Kinetically controlled glass transition measurement of organic aerosol thin films using broadband dielectric spectroscopy, Atmos. Meas. Tech., 11, 3479–3490, https://doi.org/10.5194/amt-11-3479-2018, 2018.

Zhang, Y., Nichman, L., Spencer, P., Jung, J. I., Lee, A., Heffernan, B. K., Gold, A., Zhang, Z., Chen, Y., Canagaratna, M. R., Jayne, J. T., Worsnop, D. R., Onasch, T. B., Surratt, J. D., Chandler, D., Davidovits, P. and Kolb, C. E.: The cooling rate and volatility dependent glass forming properties of organic aerosols measured by Broadband Dielectric Spectroscopy, Environ. Sci. & Technol., 53, 12366-12378, https://doi.org/10.1021/acs.est.9b03317, 2019.

Zhou, S., Hwang, B. C. H., Lakey, P. S. J., Zuend, A., Abbatt, J. P. D. and Shiraiwa, M.: Multiphase reactivity of polycyclic aromatic hydrocarbons is driven by phase separation and diffusion limitations, Proc. Natl. Acad. Sci. U.S.A., 116, 11658-11663, https://doi.org/10.1073/pnas.1902517116, 2019.

Zobrist, B., Marcolli, C., Pedernera, D. and Koop, T.: Do atmospheric aerosols form glasses?, Atmos. Chem. Phys., 8, 5221-5244, https://doi.org/10.5194/acp-8-5221-2008, 2008.

Zuend, A. and Seinfeld, J. H.: Modeling the gas-particle partitioning of secondary organic aerosol: the importance of liquid-liquid phase separation, Atmos. Chem. Phys., 12, 3857-3882, https://doi.org/10.5194/acp-12-3857-2012, 2012.

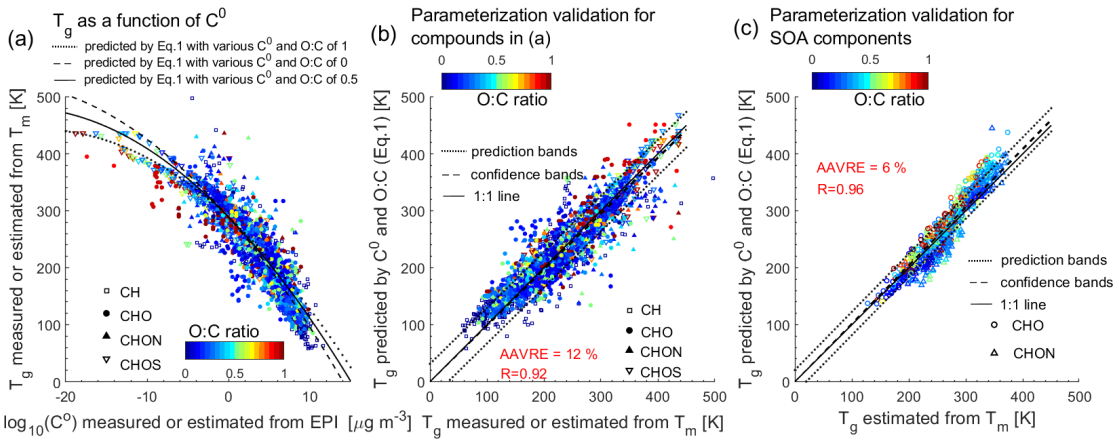

Figure 1. (a) T_g of organic compounds in the training dataset plotted against C^0. The lines show the predictions of T_g (Eq. 1) by C^0 and the O:C ratio of 0 (dashed), 0.5 (solid), and 1 (dotted). (b) Predicted T_g by C^0 and the O:C ratio (Eq. 1) for compounds shown in (a) compared to measured or otherwise estimated T_g from T_m. (c) Predicted T_g for SOA components (Shiraiwa et al., 2014) using Eq. (1) plotted against estimated T_g from T_m with the Boyer-Kauzmann rule. The correlation coefficient (R) and the average absolute value of the relative error (AAVRE) are shown. The dashed and dotted lines in (b) and (c) show 68% confidence and prediction bands, respectively.

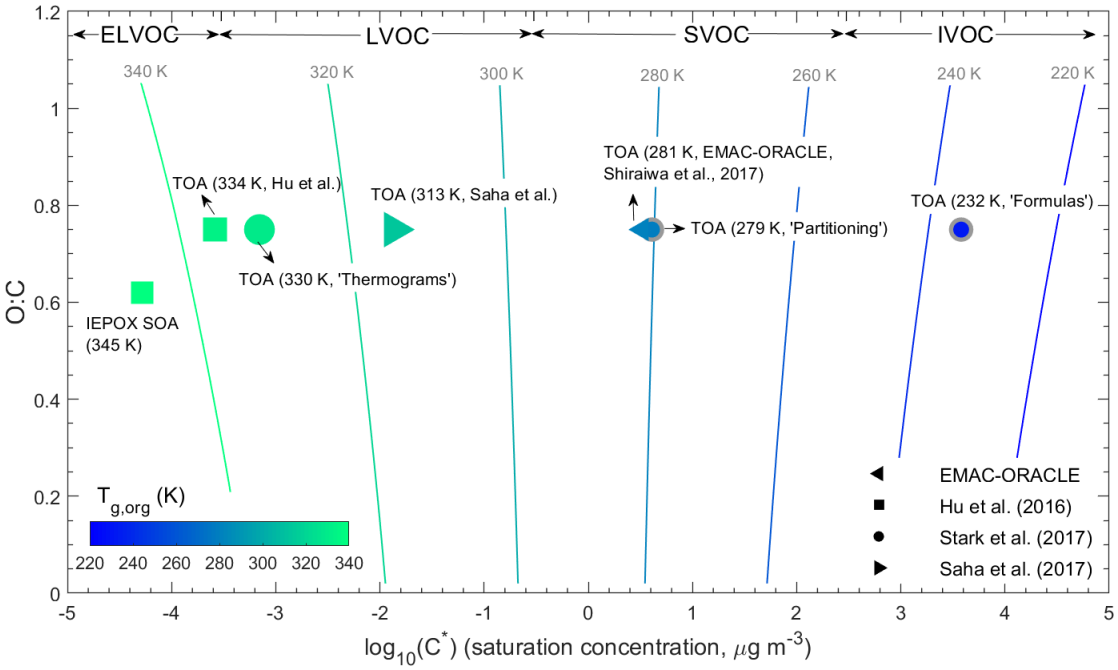

Figure 2. Predicted glass transition temperatures of organic aerosols under dry conditions ($T_{g,org}$) during the SOAS campaign placed into the 2-D VBS framework. The isopleths correspond to the T_g calculated using Eq. (1) with the effective saturation mass concentration (C^*) and the O:C ratio defined in the 2D-VBS. The markers represent the $T_{g,org}$ of total OA (TOA) and IEPOX SOA calculated from the volatility distributions simulated by a global chemical transport model EMAC-ORACLE (Shiraiwa et al., 2017) or measured during the SOAS campaign (Hu et al., 2016; Saha et al., 2017; Stark et al., 2017). Three methods ('Formulas', 'Partitioning', and 'Thermograms') are applied in Stark et al. (2017) to derive the C^* distributions, while the "Thermograms" method provides the most credible volatility distributions compared to 'Formulas' and 'Partitioning' (marker edge lines in gray).

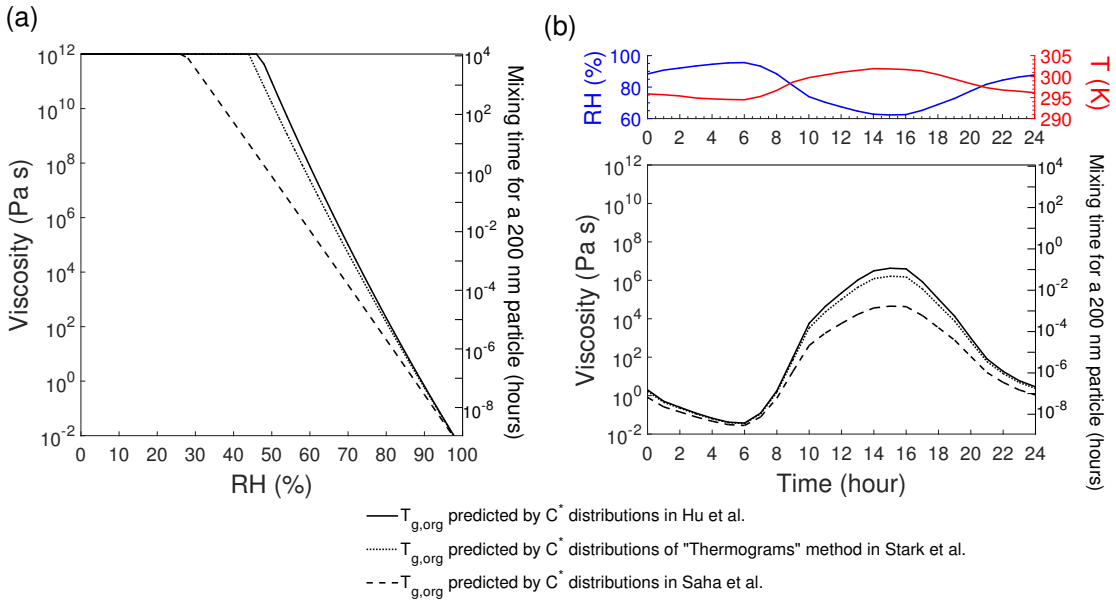

Figure 3. (a) Predicted viscosity of total OA measured during the SOAS campaign as a function of RH. (b) Diurnal variations of viscosity of total OA predicted employing the measured RH and T (Hu et al., 2016) during the SOAS campaign. $T_{g,org}$ are calculated using the volatility distributions measured in Hu et al., (2016), Saha et al. (2017), and the "Thermograms" method in Stark et al. (2017). Characteristic mixing timescales of organic molecules with the radius of 10^{-10} m within 200 nm particles are also shown in the right axis.

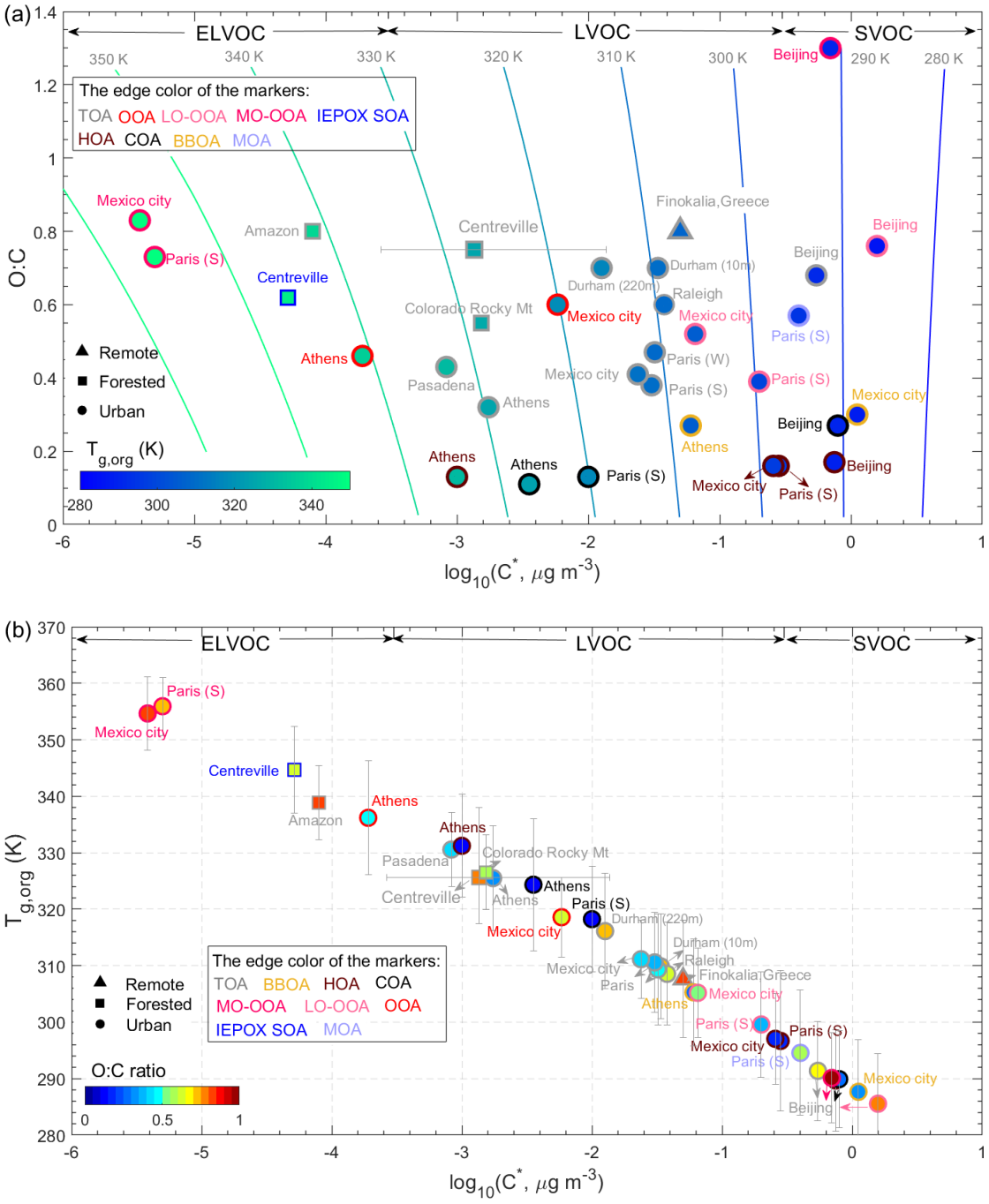

Figure 4. Predicted glass transition temperatures of organic aerosols under dry conditions ($T_{g,org}$) at 11 sites. The fill color of the markers represents $T_{g,org}$ (a) or the O:C ratio (b). The marker edge color indicates the OA components identified via PMF of the AMS mass spectra. The isopleths in (a) correspond to T_g calculated using Eq. (1) with C^* and O:C defined in the 2D-VBS. The vertical error bars correspond to uncertainties in $T_{g,org}$ considering parameterization uncertainties and error propagation. The horizontal error bars for the Centreville site correspond to the upper and lower limits of the average $\log_{10}(C^*)$ calculated from different volatility distributions measured during the SOAS campaign (Hu et al., 2016; Saha et al., 2017; Stark et al., 2017).

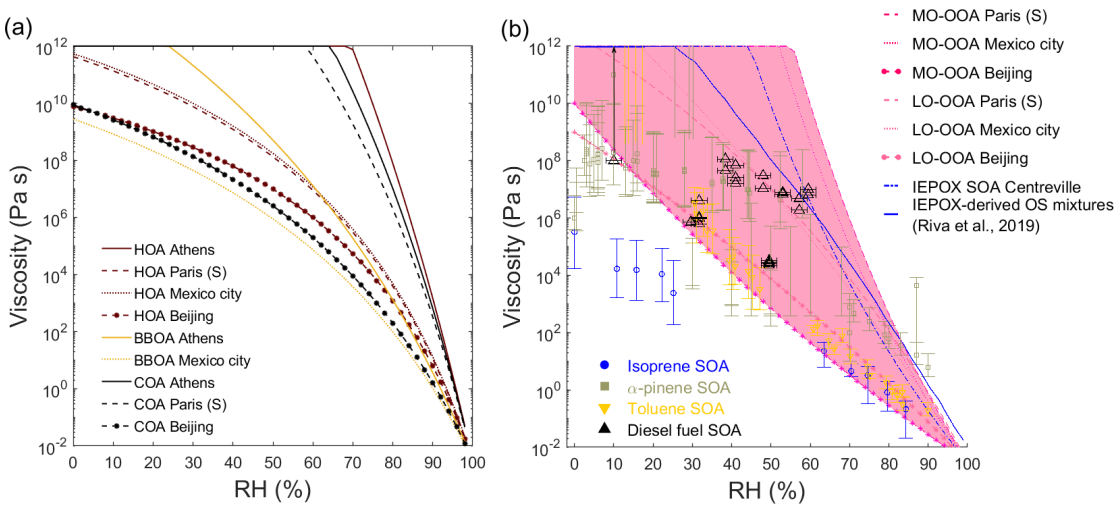

Figure 5. Predicted viscosity of (a) HOA, COA and BBOA and (b) LO-OOA, MO-OOA, and IEPOX SOA in different locations at 298 K as a function of RH. Experimentally measured viscosity of laboratory-generated SOA formed from isoprene (Song et al., 2015), α-pinene (Abramson et al., 2013; Renbaum-Wolff et al., 2013; Kidd et al., 2014; Pajunoja et al., 2014; Bateman et al., 2015; Zhang et al., 2015; Grayson et al., 2016; Petters et al., 2019), toluene (Song et al., 2016), and diesel fuel (Song et al., 2019) are also shown. Predicted viscosity of IEPOX-derived OS mixtures (solid blue line) is from Riva et al. (2019). Note that in case these OA factors are internally mixed with other components, the predicted viscosity would not represent real ambient complex organic mixtures.

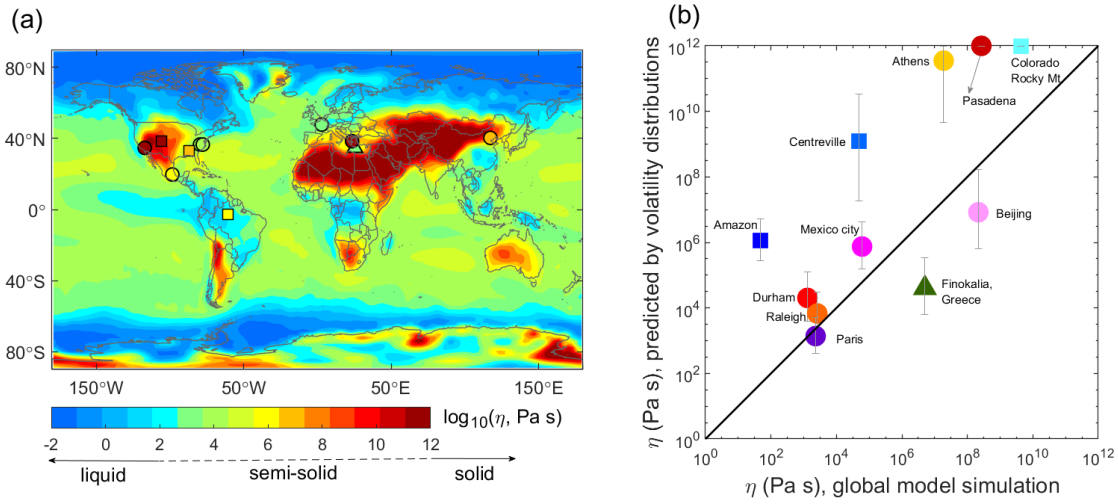

Figure 6. (a) Global distributions of SOA annually averaged viscosity at the surface simulated by a global chemical transport model (Shiraiwa et al., 2017) with the viscosity predicted by measured volatility distributions at 11 global sites (triangle, square and circle represent remote, forested and urban sites, respectively, Table S3). The color code indicates viscosity in a log scale. (b) Predicted viscosity based on measured volatility distributions compared against the viscosity in global simulations. The error bars correspond to uncertainties in viscosities calculated from uncertainties in predicted $T_{g,org}$ shown in Fig. 4.

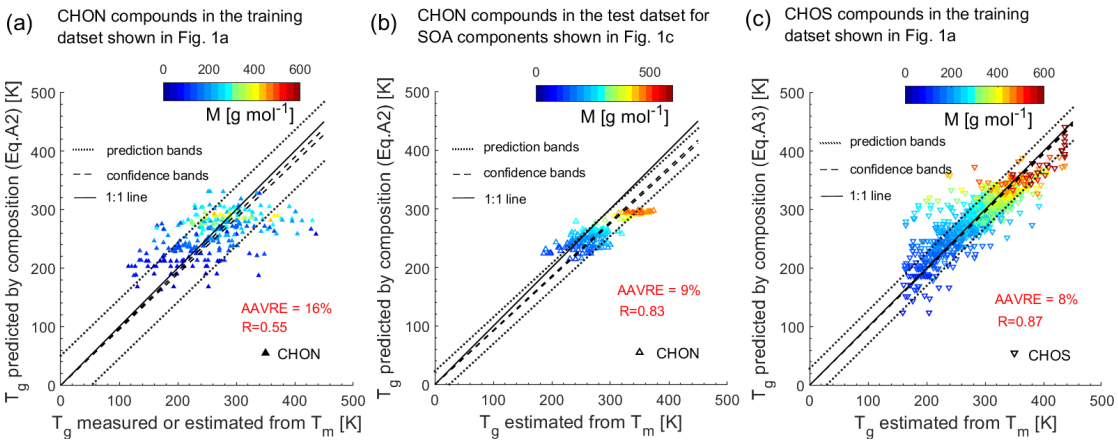

Figure A1. T_g predicted by elemental composition (Eq. A2) compared to (a) measured or otherwise estimated T_g by the Boyer-Kauzmann rule using measured T_m for CHON compounds in the training dataset and (b) estimated T_g by the Boyer-Kauzmann rule with T_m estimated by the EPI suite for CHON compounds in the test dataset for SOA components. (c) T_g predicted by elemental composition (Eq. A3) compared to estimated T_g by the Boyer-Kauzmann rule with T_m estimated by the EPI suite for CHOS compounds in the training dataset. The dashed and dotted lines show 68% confidence and prediction bands, respectively. The correlation coefficient (R) and the average absolute value of the relative error (AAVRE) are included in each figure legend.

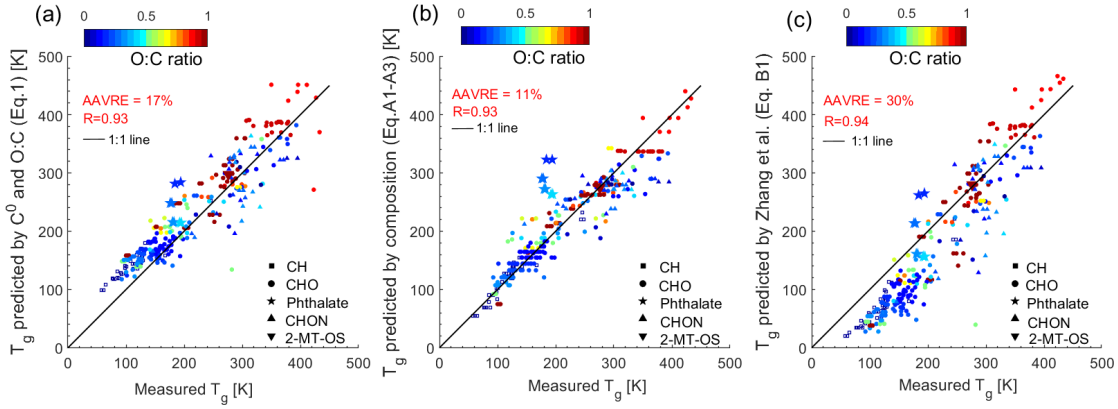

Figure B1. Comparison between measured T_g in the training dataset in Fig. 1a and T_g predicted by (a) C^0 and O:C (Eq. 1), (b) elemental composition (Eqs. A1-A3), and (c) the parameterization (Eq. B1) in Zhang et al. (2019). The solid line shows the 1:1 line. The correlation coefficient (R) and the average absolute value of the relative error (AAVRE) are included in each figure legend.

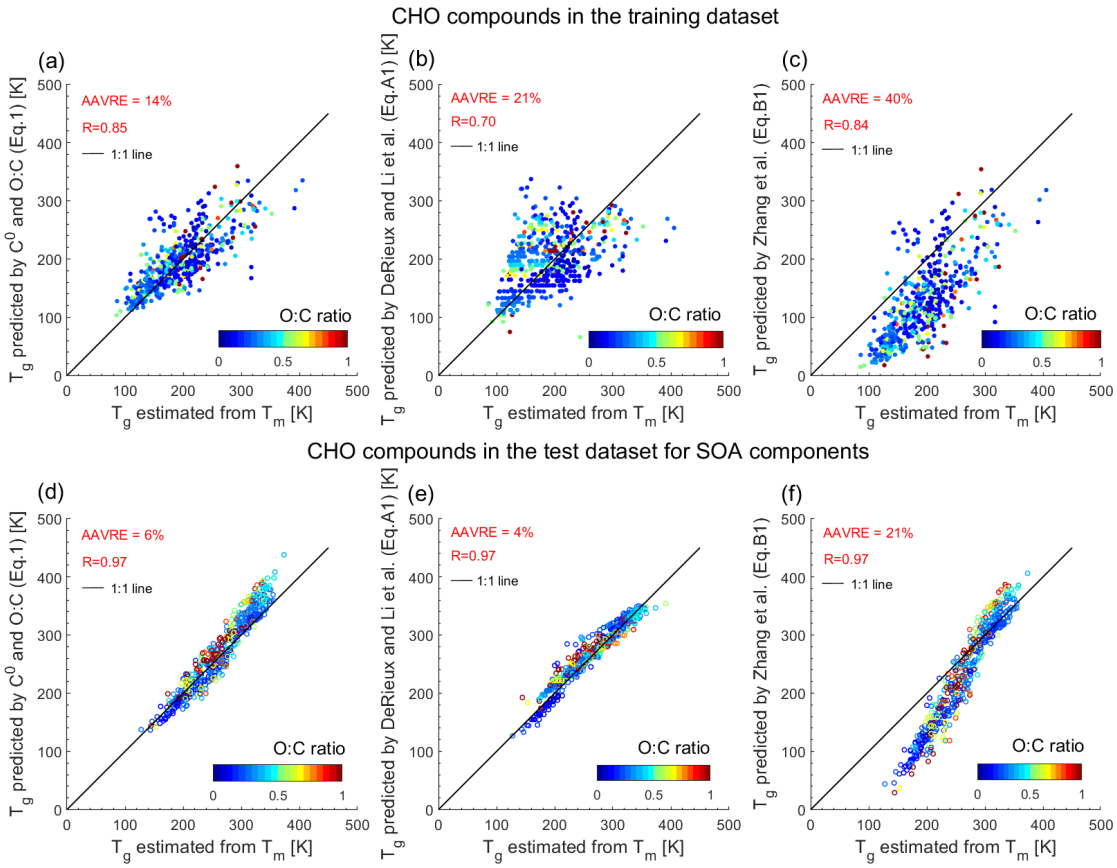

Figure B2. Predicted T_g by (a) C^0 and O:C (Eq. 1), (b) elemental composition (Eq. A1), and (c) the parameterization (Eq. B1) in Zhang et al. (2019) plotted against estimated T_g from T_m applying the Boyer-Kauzmann rule. CHO compounds in (a) – (c) included in the training dataset shown in Fig. 1a are with measured T_m and C^0 values; CHO compounds in (d) – (f) included in the test dataset for SOA components shown in Fig. 1c are with T_m and C^0 values estimated by the EPI Suite and the EVAPORATION model, respectively. The correlation coefficient (R) and the average absolute value of the relative error (AAVRE) are shown.

Supplement of

Predictions of the glass transition temperature and viscosity of organic aerosols from volatility distributions

Ying Li[1,*], Douglas A. Day[2,3], Harald Stark[2,3,4], Jose L. Jimenez[2,3] and Manabu Shiraiwa[1,*]

[1] Department of Chemistry, University of California, Irvine, CA 92697-2025, USA

[2] Cooperative Institute for Research in Environmental Sciences (CIRES), University of Colorado, Boulder, CO 80309, USA

[3] Department of Chemistry, University of Colorado, Boulder, CO 80309, USA

[4] Aerodyne Research Inc., Billerica, Massachusetts 01821, USA

[*]Correspondence to: Ying Li (yingl47@uci.edu) or Manabu Shiraiwa (m.shiraiwa@uci.edu)

To be submitted to Atmospheric Chemistry and Physics Discussions (ACPD)

Table S1. Number of the compounds included in the training dataset and their T_g, C^0 and T_m measured or otherwise estimated.

	CH	CHO	CHON	CHOS
Both T_g and C^0 measured	38	125	5	0
Measured T_g, C^0 estimated from EPI Suite	4	134	30	1
T_g estimated from measured T_m, measured C^0	391	537	241	18
T_g estimated from T_m, T_m estimated from EPI Suite, measured C^0	0	0	0	11
T_g estimated from measured T_m, C^0 estimated from EPI Suite	0	0	0	63
T_g estimated from T_m, T_m and C^0 estimated from EPI Suite	0	0	0	850

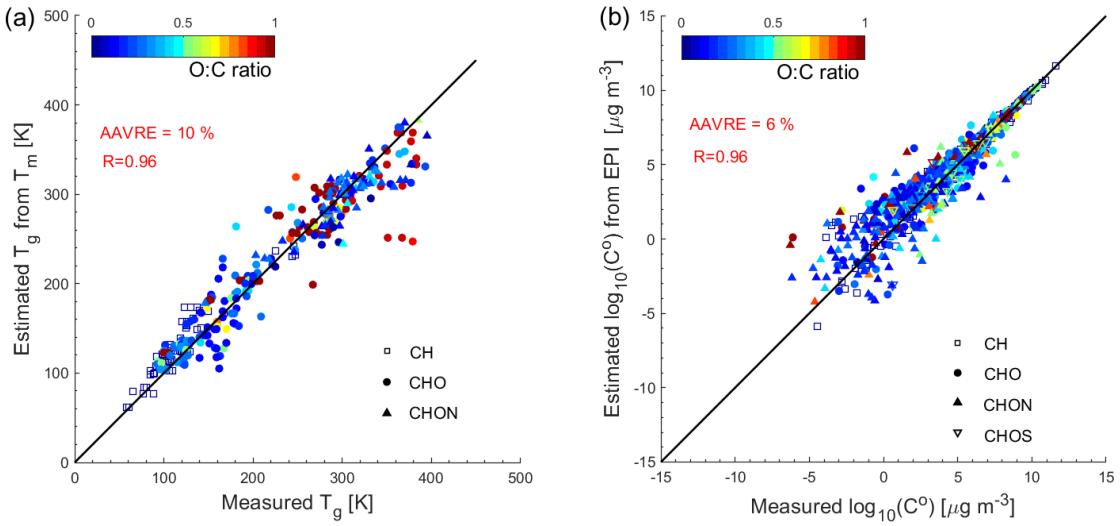

Figure S1. (a) Comparison of the measured T_g (Koop et al., 2011; Dette et al., 2014; Rothfuss and Petters, 2017; Lessmeier et al., 2018; Zhang et al., 2019) and the T_g estimated by the Boyer–Kauzmann rule for 336 organic compounds with their measured T_m available. (b) Comparison of pure compound saturation mass concentration (C^0) measured and estimated from the EPI suite for 1637 organic compounds included in the training dataset.

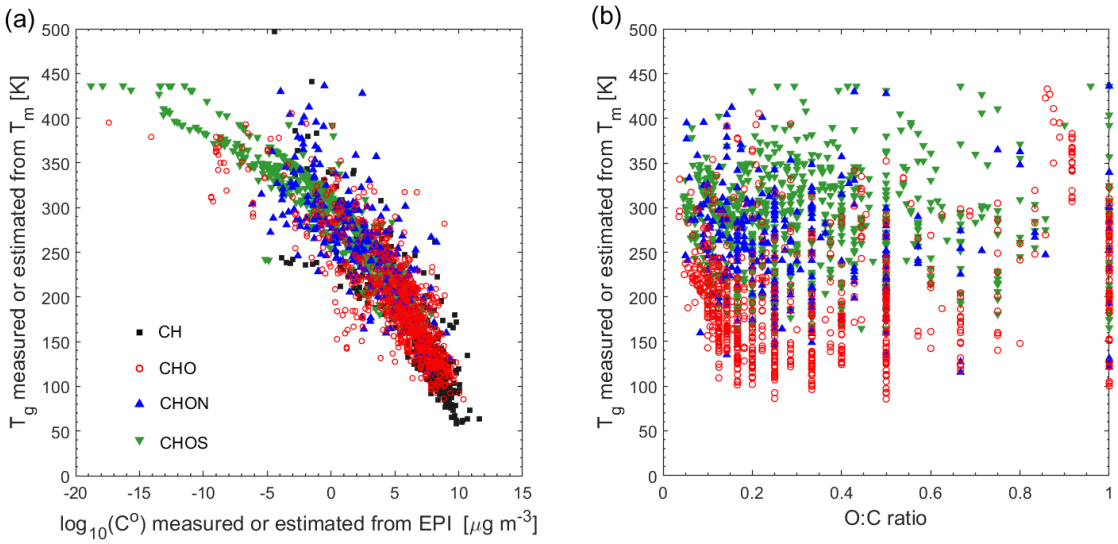

Figure S2. T_g of organic compounds in the training dataset plotted against (a) pure compound saturation mass concentration (C^0) and (b) the atomic O:C ratio.

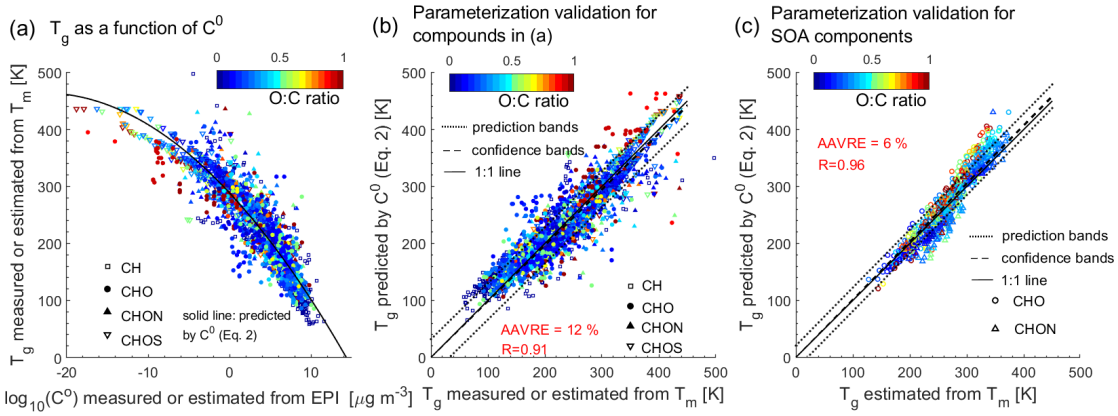

Figure S3. (a) T_g of organic compounds in the training dataset plotted against C^0. The solid line shows the predictions of T_g by C^0 (Eq. 2). (b) Predicted T_g by C^0 (Eq. 2) for compounds shown in (a) compared to measured or otherwise estimated T_g from T_m. (c) Predicted T_g for SOA components (Shiraiwa et al., 2014) using Eq. (2) plotted against estimated T_g from T_m with the Boyer-Kauzmann rule. The correlation coefficient (R) and the average absolute value of the relative error (AAVRE) are shown. The dashed and dotted lines in (b) and (c) show 68% confidence and prediction bands, respectively.

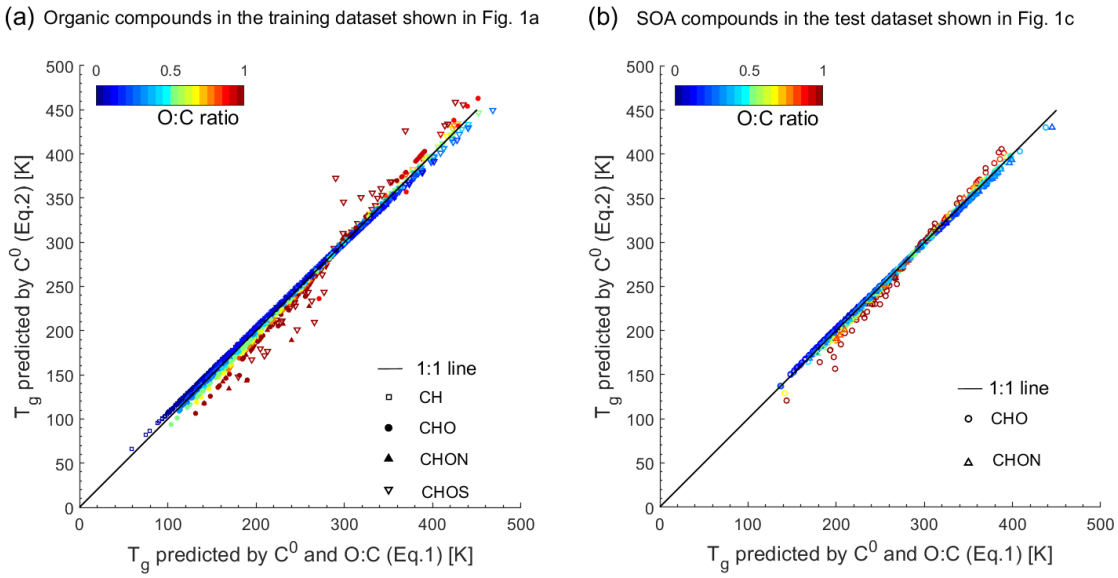

Figure S4. T_g predicted as a function of C^0 using Eq. (2) compared to T_g predicted as a function of C^0 and the O:C ratio using Eq. (1) for (a) organic compounds included in the training dataset and (b) SOA components (Shiraiwa et al., 2014) in the test dataset.

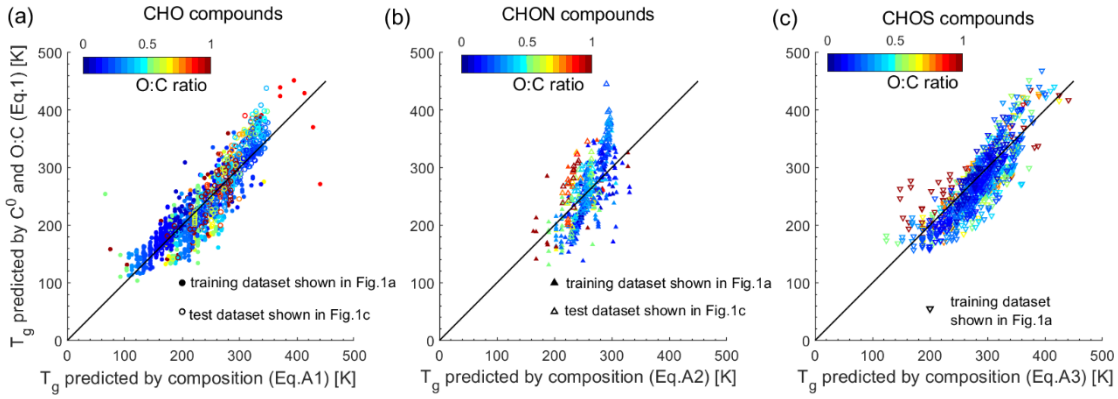

Figure S5. T_g predicted as a function of C^0 and the O:C ratio using Eq. (1) compared to T_g predicted as a function of elemental compositions using (a) Eq. (A1) for CHO compounds, (b) Eq. (A2) for CHON compounds, and (c) Eq. (A3) for CHOS compounds. The solid line shows the 1:1 line.

References:

Dette, H. P., Qi, M., Schröder, D. C., Godt, A. and Koop, T.: Glass-forming properties of 3-methylbutane-1,2,3-tricarboxylic acid and its mixtures with water and pinonic acid, J. Phys. Chem. A, 118, 7024-7033, https://doi.org/10.1021/jp505910w, 2014.

Koop, T., Bookhold, J., Shiraiwa, M. and Poschl, U.: Glass transition and phase state of organic compounds: dependency on molecular properties and implications for secondary organic aerosols in the atmosphere, Phys. Chem. Chem. Phys., 13, 19238-19255, 10.1039/C1CP22617G, 2011.

Lessmeier, J., Dette, H. P., Godt, A. and Koop, T.: Physical state of 2-methylbutane-1,2,3,4-tetraol in pure and internally mixed aerosols, Atmos. Chem. Phys., 18, 15841-15857, 10.5194/acp-18-15841-2018, 2018.

Rothfuss, N. E. and Petters, M. D.: Influence of Functional Groups on the Viscosity of Organic Aerosol, Environ. Sci. Technol., 51, 271-279, 10.1021/acs.est.6b04478, 2017.

Shiraiwa, M., Berkemeier, T., Schilling-Fahnestock, K. A., Seinfeld, J. H. and Pöschl, U.: Molecular corridors and kinetic regimes in the multiphase chemical evolution of secondary organic aerosol, Atmos. Chem. Phys., 14, 8323-8341, 10.5194/acp-14-8323-2014, 2014.

Zhang, Y., Nichman, L., Spencer, P., Jung, J. I., Lee, A., Heffernan, B. K., Gold, A., Zhang, Z., Chen, Y., Canagaratna, M. R., Jayne, J. T., Worsnop, D. R., Onasch, T. B., Surratt, J. D., Chandler, D., Davidovits, P. and Kolb, C. E.: The cooling rate and volatility dependent glass forming properties of organic aerosols measured by Broadband Dielectric Spectroscopy, Environ. Sci. & Technol., 53, 12366-12378, https://doi.org/10.1021/acs.est.9b03317, 2019.